Earth Syst. Sci. Data, 10, 87–107, 2018
https://doi.org/10.5194/essd-10-87-2018

Open Access Earth System Science Data

The Open-source Data Inventory for Anthropogenic CO_2, version 2016 (ODIAC2016): a global monthly fossil fuel CO_2 gridded emissions data product for tracer transport simulations and surface flux inversions

Tomohiro Oda[1,2], Shamil Maksyutov[3], and Robert J. Andres[4]

[1]Global Modeling and Assimilation Office, NASA Goddard Space Flight Center, Greenbelt, MD, USA
[2]Goddard Earth Sciences Technology and Research, Universities Space Research Association, Columbia, MD, USA
[3]Center for Global Environmental Research, National Institute for Environmental Studies, Tsukuba, Ibaraki, Japan
[4]Carbon Dioxide Information Analysis Center, Oak Ridge National Laboratory, Oak Ridge, TN, USA

Correspondence: Tomohiro Oda (tomohiro.oda@nasa.gov)

Received: 18 July 2017 – Discussion started: 20 July 2017
Revised: 20 November 2017 – Accepted: 22 November 2017 – Published: 18 January 2018

Abstract. The Open-source Data Inventory for Anthropogenic CO_2 (ODIAC) is a global high-spatial-resolution gridded emissions data product that distributes carbon dioxide (CO_2) emissions from fossil fuel combustion. The emissions spatial distributions are estimated at a 1×1 km spatial resolution over land using power plant profiles (emissions intensity and geographical location) and satellite-observed nighttime lights. This paper describes the year 2016 version of the ODIAC emissions data product (ODIAC2016) and presents analyses that help guide data users, especially for atmospheric CO_2 tracer transport simulations and flux inversion analysis. Since the original publication in 2011, we have made modifications to our emissions modeling framework in order to deliver a comprehensive global gridded emissions data product. Major changes from the 2011 publication are (1) the use of emissions estimates made by the Carbon Dioxide Information Analysis Center (CDIAC) at the Oak Ridge National Laboratory (ORNL) by fuel type (solid, liquid, gas, cement manufacturing, gas flaring, and international aviation and marine bunkers); (2) the use of multiple spatial emissions proxies by fuel type such as (a) nighttime light data specific to gas flaring and (b) ship/aircraft fleet tracks; and (3) the inclusion of emissions temporal variations. Using global fuel consumption data, we extrapolated the CDIAC emissions estimates for the recent years and produced the ODIAC2016 emissions data product that covers 2000–2015. Our emissions data can be viewed as an extended version of CDIAC gridded emissions data product, which should allow data users to impose global fossil fuel emissions in a more comprehensive manner than the original CDIAC product. Our new emissions modeling framework allows us to produce future versions of the ODIAC emissions data product with a timely update. Such capability has become more significant given the CDIAC/ORNL's shutdown. The ODIAC data product could play an important role in supporting carbon cycle science, especially modeling studies with space-based CO_2 data collected in near real time by ongoing carbon observing missions such as the Japanese Greenhouse gases Observing SATellite (GOSAT), NASA's Orbiting Carbon Observatory-2 (OCO-2), and upcoming future missions. The ODIAC emissions data product including the latest version of the ODIAC emissions data (ODIAC2017, 2000–2016) is distributed from http://db.cger.nies.go.jp/dataset/ODIAC/ with a DOI (https://doi.org/10.17595/20170411.001).

Published by Copernicus Publications.

1 Introduction

Carbon dioxide (CO_2) emissions from fossil fuel combustion are the main cause for the observed increase in atmospheric CO_2 concentration. The Carbon Dioxide Information Analysis Center (CDIAC) at the Oak Ridge National Laboratory (ORNL) estimated that the global total fossil fuel CO_2 emissions (FFCO2; fuel combustion, cement production, and gas flaring) in the year 2014 was 9.855 PgC based on fuel statistics data published by the United Nations, UN (Boden et al., 2017). This FFCO2 estimate often serves as a reference in carbon budget analysis, especially for inferring CO_2 uptake by the terrestrial biosphere and oceans (e.g., Ballantyne et al., 2012; Le Quéré et al., 2016). The Global Carbon Project (GCP), for example, estimated that approximately 55 % of the carbon released to the atmosphere (FFCO2 plus emissions from land use change) was taken up by natural sinks over the past decade (2006–2015) (Le Quéré et al., 2016).

Similarly, FFCO2 estimates serve as a reference in atmospheric CO_2 flux inversion analysis in which the location and size of natural sources and sinks are estimated using atmospheric CO_2 data and atmospheric transport models (e.g., Tans et al., 1990; Bousquet et al., 1999; Gurney et al., 2002; Baker et al., 2006). In the conventional inversion method, unlike land and oceanic fluxes, FFCO2 is a given quantity and never optimized (e.g., Gurney et al., 2005). FFCO2 thus needs to be accurately quantified and given in space and time to yield robust estimates of natural fluxes (Gurney et al., 2005). Accurately prescribing FFCO2 has become more critical because of the use of spatially and temporally dense CO_2 data from a wide variety of observational platforms (ground-based, aircraft, and satellites), which inform not only background levels of CO_2 concentration but also CO_2 contributions from anthropogenic sources (e.g., Schneising et al., 2013; Janardanan et al., 2016; Hakkarainen et al., 2016). Atmospheric transport models then need to be run at a higher spatiotemporal resolution than before to fully interpret and utilize CO_2 variability observed on a synoptic to local scale to quantify sources and sinks (e.g., L. Feng et al., 2016; Lauvaux et al., 2016). FFCO2 data thus need to be accurately given at a high resolution so as not to cause biases in simulations.

Global FFCO2 data are available in a gridded form from different institutions and research groups (e.g., CDIAC/ORNL and Europe's Joint Research Centre, JRC) and those gridded emissions data are often based on disaggregation of national (or sectoral) emissions (e.g., Andres et al., 1996; Rayner et al., 2010; Oda and Maksyutov, 2011; Janssens-Maenhout et al., 2012; Kurokawa et al., 2013; Asefi-Najafabady et al., 2014). The emissions spatial distributions are often estimated using spatial proxy data that approximate the location and intensity of human activities (hence, CO_2 emissions) (e.g., population, nighttime lights, and gross domestic production, GDP) and/or geolocation of specific emissions sources (e.g., power plant, transportation, cement production/industrial facilities, and gas flares). The CDIAC gridded emissions data product, for example, is based on an emissions disaggregation using population density at a $1 \times 1^\circ$ resolution (Andres et al., 1996). The Emission Database for Global Atmospheric Research (EDGAR, http://edgar.jrc.ec.europa.eu/) estimates emissions on the emissions sectors specified by the Intergovernmental Panel on Climate Change (IPCC) methodology instead of fuel type and it uses spatial proxy data and geospatial data such as point and line source location at a $0.1 \times 0.1^\circ$ resolution (Janssens-Maenhout et al., 2012).

Satellite-observed nighttime light data have been identified as an excellent spatial indicator for human settlements and intensities of some specific human activities (e.g., Elvidge et al., 1999, 2009) and have been used to infer the associated CO_2 emissions or their spatial distributions (e.g., Doll et al., 2000; Ghosh et al., 2010; Rayner et al., 2010). Oda and Maksyutov (2011) proposed a combined use of power plant profiles (power plant emissions intensity and geographical location) and nighttime light data to achieve a global high-spatial-resolution emissions field. The decoupling of the point source emissions, which often has less spatial correlation with population (hence, nighttime light), yields improved high-resolution emissions fields that show an improved agreement with the US 10 km Vulcan emissions product developed by Gurney et al. (2009) (Oda and Maksyutov, 2011). Based on Oda and Maksyutov (2011), we initiated the high-resolution emissions data development (named the Open-source Data Inventory for Anthropogenic CO_2, ODIAC) under the Japanese Greenhouse gases Observing SATellite (GOSAT; Yokota et al., 2009) project at the Japanese National Institute for Environmental Studies (NIES). The original purpose of the emissions data development was to provide an accurate prior FFCO2 field for global and regional CO_2 inversions using the column-averaged CO_2 (X_{CO_2}) data collected by GOSAT. Since 2009, the ODIAC emissions data product has been used for the inversion for the official GOSAT Level 4 (surface CO_2 flux) data production (Takagi et al., 2009; Maksyutov et al., 2013), NOAA's CarbonTracker (Peters et al., 2007) as supplementary FFCO2 data, and dozens of published works (e.g., Saeki et al., 2013; Thompson et al., 2016; S. Feng et al., 2016, 2017; Shirai et al., 2017) including several urban scale modeling studies (e.g., Ganshin et al. 2012; Oda et al., 2012, 2017; Brioude et al., 2013; Lauvaux et al., 2016; Janardanan et al., 2016).

In response to increasing needs from the CO_2 modeling research community, we have upgraded and modified our modeling framework in order to produce a global, comprehensive emissions data product in a timely manner, while our flagship high-resolution emissions modeling approach remains the same. In this paper, we describe the year 2016 version of the ODIAC emissions data product (ODIAC2016, 2000–2015), which was the latest version of the ODIAC emissions data at the time of the submission of this paper, along with the emissions modeling framework we are currently

based on, highlighting changes and differences from Oda and Maksyutov (2011). Currently, the updated 2017 version of the ODIAC emissions data (ODIAC2017, 2000–2016) is available. Although this paper describes ODIAC2016, the readers should be able to understand how we developed ODIAC2017 (the latest) with updated information.

2 Emissions modeling framework

Figure 1 illustrates our current ODIAC emissions modeling framework (we defined it as "ODIAC 3.0 model", in contrast to the original version). Major changes and differences from Oda and Maksyutov (2011, ODIAC v1.7) are (1) the use of emissions estimates made by the CDIAC/ORNL (rather than our own emissions estimates), (2) the use of multiple spatial emissions proxies in order to distribute CDIAC national emissions estimates made by fuel type, and (3) the inclusion of emissions temporal variations (version 1.7 only indicates annual emissions fields). Given that CDIAC emissions estimates have been well-respected and widely used in the carbon research community (e.g., Ballantyne et al., 2012; Le Quéré et al., 2016), our mission in our emissions data development is to develop and deliver an extended, comprehensive global gridded emissions data product, fully utilizing CDIAC emissions data (e.g., emissions estimates in both tabular and gridded forms). We also extend CDIAC emissions data where possible. Our emissions modeling framework was also designed to produce an annually updated emissions data product in a timely manner. Given the discontinuity of future updated CDIAC emissions data, we believe that our capability of producing an extended product of the CDIAC emissions data is significant.

Starting with national emissions estimates as an input, our model framework achieves monthly, global FFCO2 gridded fields via preprocessing and spatial and temporal disaggregation. CDIAC national estimates made by fuel type (liquid, gas, solid, cement production, gas flare, and international bunker emissions) are further divided into an extended set of ODIAC emissions categories (point source, nonpoint source, cement production, gas flare, international aviation, and marine bunkers; further described in Sect. 3). It is important to note that ODIAC2016 carries emissions from international bunkers (international marine bunkers and aviation often account for a few percent of the global total emissions), which are not included in the CDIAC gridded emissions data products (CDIAC gridded emissions data only indicate national emissions and international bunker emissions are often not considered to be a part of national emissions in an international convention). With the inclusion of international bunker emissions, we provide a more comprehensive global gridded emissions field. We extended the CDIAC national estimates over the recent years that were not yet covered in the previous version of CDIAC gridded data (2014–2016) in order to support near-real time CO_2 simulations and analysis. Emissions are then spatially distributed using a wide variety of spatial data (e.g., point source geographical location, nighttime light data, and flight and ship tracks; further described in Sect. 4). We adopt an emissions seasonality from existing emissions inventories for particular emissions categories (further described in Sect. 5).

In the following sections (Sects. 3–5), we describe how ODIAC2016 was developed. It is important to note that ODIAC2016 is based on the best available data at the time of the development (ODIAC2016 was released in September 2016). Thus, some of the emissions estimates and underlying data used in ODIAC2016 might now be outdated. For traceability purposes, data used in this development, their versions or editions, and data sources are summarized in Table A1 in the Appendix. Following the results and evaluation section (Sect. 6), we discuss caveats and current limitations in our modeling framework and emissions data product (Sect. 7), and then we describe how we will update the ODIAC emissions data product with updated fuel statistics and/or emissions information (Sect. 8). Recently published atmospheric CO_2 inversion studies (e.g., Maksyutov et al., 2013) and operational assimilation systems such as NOAA's CarbonTracker (https://www.esrl.noaa.gov/gmd/ccgg/carbontracker/) often focus on time periods after 2000. We thus made it a priority to produce emissions data after the year 2000 with regular update upon the availability of updated emissions and fuel statistical data and deliver the emissions product to the science community, instead of developing a longer-term emissions data product. Future versions of ODIAC data, however, might have longer, extended time coverage. Currently the ODIAC data are provided in two data formats: (1) global 1×1 km (30 arcsec) monthly data in the GeoTIFF format (only includes emissions over land) and (2) $1 \times 1^\circ$ annual (12 month) data in the NetCDF format (includes international bunker emissions). The $1 \times 1^\circ$ annual data are aggregated from the 1×1 km product. The improvements with the use of improved nighttime light data in the 1×1 km data were documented in Oda et al. (2012). This paper thus focuses on the comprehensive global FFCO2 fields at a $1 \times 1^\circ$ resolution, unless otherwise specified.

3 Emissions estimates and input emissions data preprocessing

3.1 Emissions for 2000–2013

CDIAC FFCO2 emissions estimates are based on fuel statistic data published as the United Nation Energy Statistics Database (Boden et al., 2017). Emissions estimates are calculated on a global, national, and regional basis and by fuel type in the method described in Marland and Rotty (1984). CDIAC also provides their own gridded emissions data products that indicate annual and monthly FFCO2 fields at a $1 \times 1^\circ$ resolution (Andres et al., 1996, 2011). ODIAC2016 is primarily based on the year 2016 version of the CDIAC

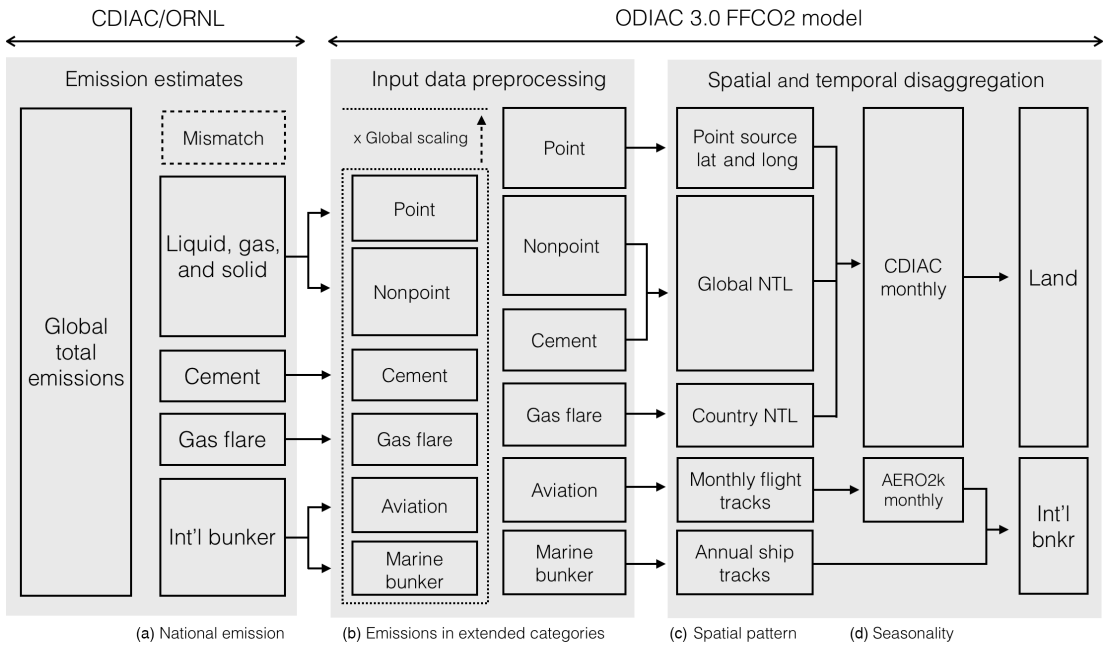

Figure 1. A schematic figure of the ODIAC emissions modeling framework (defined as "ODIAC 3.0 FFCO2 model"). Starting with CDIAC national emissions estimates made by fuel type (emissions estimates), the CDIAC national emissions estimates are first divided into extended ODIAC emissions categories (input data processing; see Sect. 3). The ODIAC 3.0 FFCO2 model then distributes the emissions in space and time, using point source geolocation information and spatial data depending on emissions categories such as nighttime light (NTL) and aircraft and ship fleet tracks (spatial disaggregation; see Sect. 4). The emissions seasonality for emissions over land and international aviation were adopted from existing emissions inventories (temporal disaggregation; see Sect. 5).

national estimates (Boden et al., 2016), which were the most up-to-date CDIAC emissions estimates at the time of the data development (currently Boden et al., 2017, is the latest). We first aggregated the CDIAC national (and regional) emissions estimates to 65 countries and 6 geographical regions (North America, South and Central America, Europe and Eurasia, the Middle East, Africa, and Asia Pacific) defined in Oda and Maksyutov (2011) (see the country/region definitions are shown in Table 1 in Oda and Maksyutov, 2011). In addition to the national and geographical categories, we decided to include Antarctic fishery emissions, which are from fishery activities over the Antarctic Ocean ($< 60°$ S, 1–4 kTC yr^{-1} over 1987–2007 by Boden et al., 2016), as an individual emissions region and distributed in the same way as Andres et al. (1996). Emissions from international bunkers and aviation are not included in national emissions by international convention. Thus, CDIAC gridded emissions data products do not include the emissions from international bunkers and aviation although the CDIAC/ORNL does have records of those emissions on a national and regional basis. ODIAC2016 includes those emissions to achieve comprehensive global FFCO2 gridded emissions fields.

In CDIAC emissions estimates, the global total emissions and national total emissions are obtained using different calculation methods (global fuel production vs. apparent national fuel consumption; see Andres et al., 2012) and the CDIAC national totals do not sum to the CDIAC global total due to the difference in calculation method and inconsistencies in the underlying statistical data (e.g., import–export totals) (e.g., Andres et al., 2012). We thus calculate the difference between the global total and the sum of national totals and scaled up national totals to account for the difference. Andres et al. (2014) reported that global total emissions estimates calculated with production data (as opposed to apparent consumption data) have the smallest uncertainty (approximately 8 %; 2σ). It is thus used as the reference for global carbon budget analyses (e.g., Le Quéré et al., 2016). Inversion analysis is an extended version of the global carbon budget analysis using atmospheric models. We thus believe that imposing transport models and/or inversion models in a consistent way with the global carbon budget analysis, as Le Quéré et al. (2016) have done, has significance, although we sacrifice the accuracy of the national and regional emissions estimates. Due to the global scaling, national totals in ODIAC2016 differ from the estimates originally reported by the CDIAC/ORNL. The difference between the CDIAC global total and the sum of national emissions is often a few percent and thus the magnitude of the scaling is often within the uncertainty range of national emissions (e.g., 4.0 to 20.2 %; Andres et al., 2014). The global scaling factors derived and used in this study are presented in Table A2.

3.2 Emissions for 2014–2015

The 2016 version of the CDIAC emissions estimates only covers years to 2013 (Boden et al., 2016). We thus extrapolated the 2013 CDIAC emissions to years 2014 and 2015 using the 2016 version of the BP global fuel statistical data (BP, 2017). Our emissions extrapolation approach is the same as Myhre et al. (2009) and Le Quéré et al. (2016). Emissions from cement production and gas flaring (approximately 5.7 and 0.6 % of the 2013 global total; Boden et al., 2016) were assumed to be the same as those in 2013. International bunker emissions were scaled using changes in national total emissions.

3.3 CDIAC emissions sector to ODIAC emissions categories

CDIAC national emissions estimates (prepared by fuel type) were recategorized into our own ODIAC emissions categories (point source, nonpoint source, cement production, gas flare, and international aviation and marine bunkers). Following Oda and Maksyutov (2011), the sum of emissions from liquid, gas, and solid fuels was further divided into point source emissions and nonpoint source emissions. The total emissions from point sources were estimated using national total power plant emissions calculated using Carbon Monitoring for Action (CARMA; Wheeler and Ummel, 2008) (Oda and Maksyutov, 2011). As mentioned earlier, CDIAC gridded emissions data products only indicate national emissions and do not include international bunker emissions (Andres et al., 1996, 2011). In contrast, EDGAR provides bunker emissions in their gridded data product (JRC, 2017). Peylin et al. (2013) show some models include international bunker emissions and some do not, although the difference due to the inclusion–exclusion of the international bunker emissions in the prescribed emissions could be corrected afterwards (Peylin et al., 2013). In ODIAC2016, we carry CDIAC international bunker emissions reported on a country basis to achieve the complete picture of the global fossil fuel emissions. Country total bunker emissions (aviation plus marine bunkers) were distributed using spatial proxy data adopted from other emissions inventories described later (see Sect. 4.3). Although the CDIAC/ORNL does not report emissions from international aviation and marine bunkers separately, we loosely estimated those two emissions using UN statistics. We estimated the fraction of aircraft emissions using jet fuel and aviation gasoline consumption and then the international bunker emissions were divided into aircraft and marine bunker emissions.

4 Spatial emissions disaggregation

4.1 Emissions from point sources, nonpoint sources, and cement production

We define the sum of the emissions from solid, liquid, and gas fuels as land emissions (see Fig. 1). Land emissions are further divided into two emissions categories (point source emissions and nonpoint source emissions) and then distributed at a 1×1 km resolution in the ways described in Oda and Maksyutov (2011): point source emissions are mapped using power plant profiles (emissions intensity and geographical location) taken from the CARMA database (Wheeler and Ummel, 2008) and nonpoint source emissions are distributed using nighttime light data collected by Defense Meteorological Satellite Program (DMSP) satellites (e.g., Elvidge et al., 1999). To avoid difficulty in emissions disaggregation, especially over bright regions, in nighttime light data (e.g., cities), Oda and Maksyutov (2011) employed a product that does not have an instrument saturation issue rather than a regular nighttime light product. ODIAC2016 employs the latest version of the special nighttime light product (Ziskin et al., 2010). The improved nighttime light data have mitigated the underestimation of emissions over dimmer areas seen in ODIAC v1.7 (Oda et al., 2010). Nighttime light data are currently available for multiple years (1996–1997, 1999, 2000, 2002–2003, 2004, 2005–2006, and 2010). In ODIAC2016, due to the lack of information, the emissions from cement production were spatially distributed as a part of nonpoint source emissions, although those emissions should have been distributed as point sources. This needs to be fixed in future versions of ODIAC emissions data.

4.2 Emissions from gas flaring

In ODIAC v1.7, emissions from gas flaring were not considered (Oda and Maksyutov, 2011). Nighttime light pixels corresponding to gas flares often appear very bright and would result in strong point sources in emissions data (Oda and Maksyutov, 2011). We thus identified and excluded those bright gas flare pixels before distributing land emissions using another global nighttime light data product that was specifically developed for gas flares by NOAA, National Centers for Environmental Information (NCEI, formerly National Geophysical Data Center, NGDC) (Oda and Maksyutov, 2011). In ODIAC2016 we separately distributed CDIAC gas flare emissions using the 1×1 km nighttime light-based gas flare maps developed for 65 individual countries (Elvidge et al., 2009). Other than the 65 countries, the gas flare emissions were distributed as a part of land emissions.

4.3 Emissions from international aviation and marine bunkers

Emissions from international aviation and marine bunkers were distributed using aircraft and ship fleet tracks. Interna-

tional aviation emissions were distributed using the AERO2k inventory (Eyers et al., 2005). The AERO2k inventory was developed by a team at the Manchester Metropolitan University and indicates the fuel use and NO_x, CO_2, CO, hydrocarbon, and particulate emissions for 2002 and 2025 (projected) with injection height at a $1 \times 1^\circ$ spatial resolution on a monthly basis. We used their column total CO_2 emissions to distribute emissions to a single layer. International marine bunker emissions were distributed at a $0.1 \times 0.1^\circ$ resolution using an international marine bunker emissions map from EDGAR v4.1 (JRC, 2017). We decided not to adopt an international and domestic shipping (1A3d) map from EDGAR v4.2 as it includes domestic shipping emissions that we do not distinguish.

5 Temporal emissions disaggregation

The inclusion of the emissions temporal variations is often a key in transport model simulation. For CO_2 flux inversion, the potential biases in flux inverse emissions estimates due to the lack of temporal profiles were suggested by Gurney et al. (2005). In ODIAC2016, we adopt the seasonal emissions changes developed by Andres et al. (2011). The CDIAC monthly gridded data include monthly national emissions gridded at a $1 \times 1^\circ$ resolution (Andres et al., 2011). We normalized the monthly emissions fields by the annual total and applied them to our annual emissions over land. The seasonality in ODIAC2016 is based on the 2013 version of the CDIAC monthly gridded emissions. The CDIAC monthly emissions data do not cover recent years. For recent years, we created a climatological seasonality using monthly CDIAC data from 2000 to 2010 (except 2009 when economic recession happened). Due to the limited availability of monthly fuel statistical data, Andres et al. (2011) used proxy country and also seasonality allocated with Monte Carlo simulations. The years between 2000 and 2010 were the most data-rich period and the most well explained by data (see Fig. 1 in Andres et al., 2011).

Although ODIAC2016 only provides monthly emissions fields, users can derive hourly emissions by applying scaling factors developed by Nassar et al. (2013). The Temporal Improvements for Modeling Emissions by Scaling (TIMES) is a set of scaling factors that one can derive weekly emissions and diurnal emissions from with any monthly emissions data. Temporal profiles are collected from Vulcan, EDGAR, and the best available information and are gridded on a $0.25 \times 0.25^\circ$ grid (Nassar et al., 2013). TIMES also includes per capita emissions corrections for Canada (Nassar et al., 2013).

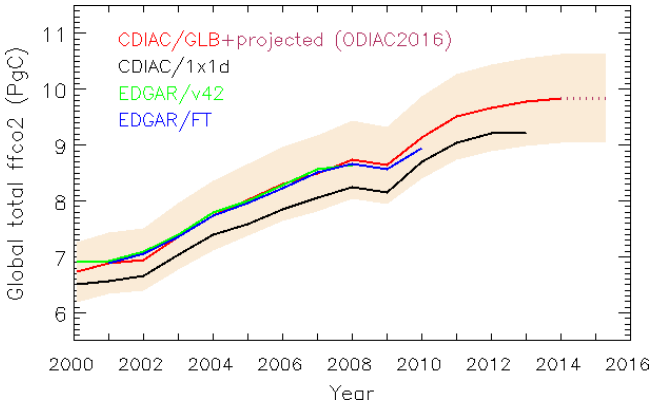

Figure 2. Global emissions time series from four gridded emissions data: CDIAC (red, 2000–2013) plus projected emissions (dashed maroon, 2014–2015) (values taken from ODIAC2016), CDIAC $1 \times 1^\circ$ (black, 2000–2013), EDGAR v4.2 (green, 2000–2008), and EDGAR v4.2 FastTrack (blue, 2000–2010). The values here are given in the unit of petagrams (equal to a gigaton) of carbon per year. The shaded area indicated in tan is the 2σ uncertainty range (8 %) estimated for CDIAC global total emissions estimates by Andres et al. (2014).

6 Results and discussions

6.1 Annual global emissions

In Fig. 2, global emissions time series from different emissions data were compared to give an idea of agreement among them. We calculated the global total for each year from four gridded emissions data for the period of 2000–2016: CDIAC global total + projection (taken from ODIAC2016), CDIAC gridded data (hence, no international bunker emissions), and two versions of EDGAR gridded data (v4.2 and FastTrack). The uncertainty range (shaded in tan) is 8 % (2σ), estimated for CDIAC global by Andres et al. (2014). Those gridded emissions data are often used in global atmospheric CO_2 inversion analysis (e.g., Peylin et al., 2013). To account for the difference in emissions reporting categories (e.g., fuel basis in CDIAC vs. emissions sector basis in EDGAR), the EDGAR totals were calculated as the total short cycle C (with the file name "CO2_excl_short-cycle_org_C") emissions minus the sum of emissions from agriculture (IPCC code: 4C and 4D), land use change and forestry (5A, C, D, F, and 4E), and waste (6C) (see more details on emissions sectors documented in JRC, 2017). International aviation (1A3a) and navigation (1A3b) were thus included in values for EDGAR time series. The authors acknowledge the JRC has updated EDGAR emissions time series for 1970–2012 in November 2014 (JRC, 2017). This study, however, uses gridded emissions data, which are not fully based on the updated emissions estimates, in order to characterize differences from gridded emissions data, especially for potential data users in the modeling community.

All four global total values obtained from four gridded emissions data agree well within 8 % uncertainty. The difference between ODIAC and CDIAC gridded data (3.3–5.7 %) was largely attributable to the international bunker emissions and global correction. ODIAC (where the total was scaled by CDIAC global total) and the two versions of EDGAR showed minor differences in magnitude (0.3–2.7 %) and trend, which are largely attributable to the differences in the underlying statistical data (e.g., UN Statistics Division vs. the US Energy Information Administration from different inventory years) and the emissions calculation method (fuel basis vs. sector basis). Global total estimates at 5-year increments are shown in Table 1. For the years 2014 and 2015, we estimated the global total emissions at 9.836 and 9.844 PgC. Boden et al. (2017) reported the latest estimate for 2014 global total emissions as 9.855 PgC. Our projected 2014 emissions estimate was lower than the latest estimate by approximately 0.02 PgC (0.2 %).

Figure 3 shows the same type of comparison as Fig. 2, but for the top 10 emitting countries (China, US, India, Russian Federation, Japan, Germany, Islamic Republic of Iran, Republic of Korea (South Korea), Saudi Arabia, and Brazil, according to the 2013 ranking reported by CDIAC). We aggregated all four gridded emissions fields to a common $1 \times 1^\circ$ field and sampled using the $1 \times 1^\circ$ country mask used in CDIAC emissions data development. The annual uncertainty estimates for national total emissions (2σ) are made following the method described by Andres et al. (2014) and values are shown in Table 2. In the analysis presented in Fig. 3, emissions from international aviation (1A3a) and navigation (1A3b) are excluded. All four national total values sampled from four gridded emissions data at a $1 \times 1^\circ$ resolution often agree within the uncertainty estimated by Andres et al. (2014). Systematic differences of ODIAC from CDIAC gridded data can be largely explained by (1) global correction (the total was scaled using CDIAC global total) and (2) the differences in emissions disaggregation methods. Although ODIAC is expected to indicate slightly higher values than CDIAC gridded data (often a few percent) because of the global correction (note global correction can be negative, despite the depiction in Fig. 1), ODIAC sometimes indicates values lower that CDIAC gridded data by more than a few percent (see Japan in Fig. 3 as an example). This is due to a sampling error using the $1 \times 1^\circ$ country map in the analysis. The aggregated $1 \times 1^\circ$ ODIAC field is slightly larger than that of CDIAC, especially because the coastal areas depicted a high resolution in the original 1×1 km emissions field. This type of sampling error was discussed in Zhang et al. (2014). ODIAC employs a 1×1 km coastline and a 5×5 km country mask as described in Oda and Maksyutov (2011). Thus, the use of a $1 \times 1^\circ$ CDIAC country map results in missing some land mass (hence, CO_2 emissions). Similar sampling errors can happen for countries that are physically small and island countries, depending on the resolution of analysis. Despite the sampling errors, the authors used the CDIAC $1 \times 1^\circ$ country map to perform this comparison analysis with CDIAC gridded data as a reference. The lower emissions indicated by ODIAC or EDGAR in this analysis do not always mean the national total emissions are lower. The emissions estimates at a national level often agree well even among different emissions inventories (e.g., Andres et al., 2012).

6.2 Global emissions spatial distributions

The global total emissions fields of CDIAC gridded emissions data and ODIAC2016 for the year 2013 (the most recent year CDIAC indicates) are shown in Fig. 4. Emissions fields are shown at a common $1 \times 1^\circ$ resolution. The major difference seen between two fields is primarily due to inclusion–exclusion of emissions from international bunker emissions that largely account for the differences indicated in Table 1. A breakdown of ODIAC 2013 emissions fields are presented by emissions category in Fig. 5. The emissions fields for point sources, nonpoint sources, cement production, and gas flaring were produced at a 1×1 km resolution in the ODIAC 3.0 model, but as mentioned earlier, we focus on the $1 \times 1^\circ$ version of ODIAC2016 in this paper. In CDIAC gridded emissions data, the emissions over land are distributed by population data without fuel type distinction. In the ODIAC 3.0 model, we have added additional layers of consideration in the emissions modeling from the conventional CDIAC model and add the possibility of future improvement with improved emissions proxy data.

In Fig. 6, we compared the four global gridded products over land and also calculated differences from ODIAC2016 (shown in Fig. 7; histograms are presented in Fig. A1). It is often very challenging to evaluate the accuracy and uncertainty of gridded emissions data because of the lack of direct physical measurements on grid scales (Andres et al., 2016). Recent studies have attempted to evaluate the uncertainty of gridded emissions data by comparing emissions data to each other (e.g., Oda et al., 2015; Hutchins et al., 2016). The differences among emissions were used as a proxy for uncertainty. However, it is important to note that such evaluation does not give us an objective measure of which one is closer to truth, beyond characterizing the differences in emissions spatial patterns and magnitudes from methodological viewpoints (e.g., emissions estimation and disaggregation). Some of the gridded emissions data are partially disaggregated using commercial information, and users are often not authorized to fully disclose the information used. This thus makes the comparison even less meaningful and/or significant. Oda et al. (2015) also discussed that emissions intercomparison approaches often do not allow us to evaluate two distinct uncertainty sources (emissions and disaggregation) separately. In addition, because of the use of emissions proxy for emissions disaggregation (rather than mechanistic modeling), such comparison can be only implemented at an aggre-

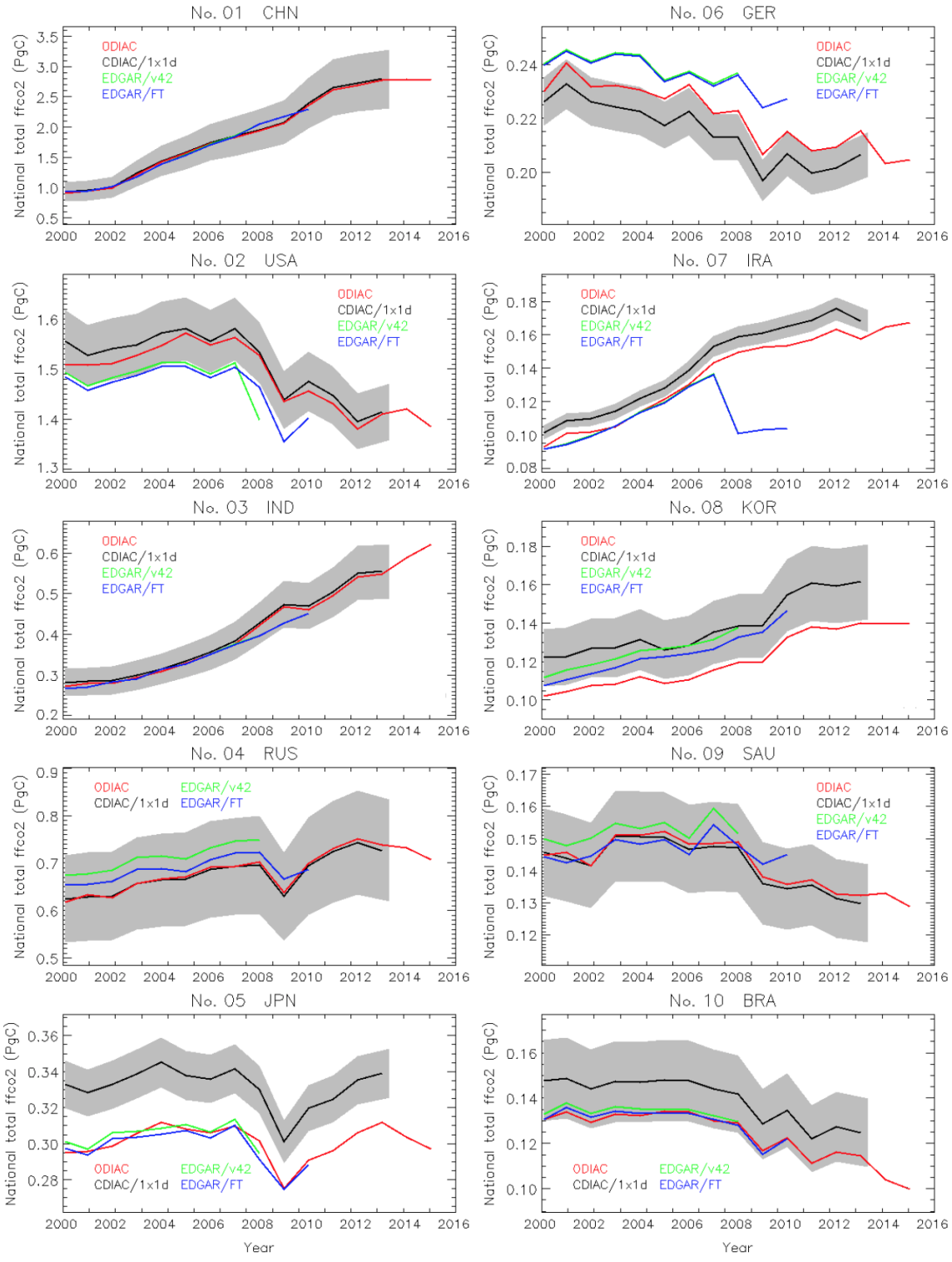

Figure 3. National emissions time series for top 10 emitting countries (China, US, India, Russian Federation, Japan, Germany, Islamic Republic of Iran, Republic of Korea (South Korea), Saudi Arabia, and Brazil). The values are given in the unit of petagrams (equal to a gigaton) of carbon per year. The values are calculated using gridded emissions data, not tabular emissions data. The national total values in the plots might thus be different from values indicated in the tabular form due to the emissions disaggregation. The shaded area in grey indicates the 2σ uncertainty range estimated by Andres et al. (2014) (see Table 2).

Table 1. Global total emissions estimates for 2000, 2005, and 2010 from four gridded emissions data estimates (ODIAC2016, CDIAC, EDGAR v4.2, and EDGAR FastTrack). Values for two versions of EDGAR emissions data were calculated by subtracting emissions from agriculture (IPCC code: 4C and 4D), land use change and forestry (5A, C, D, F, and 4E), and waste (6C) from the total EDGAR CO_2 emissions (total short cycle C).

Year	ODIAC2016	CDIAC national	EDGAR v4.2	EDGAR FT
2000	6727	6506 (−3.3 %)	6907 (+2.7 %)	NA
2005	8025	7592 (−5.4 %)	8005 (−0.2 %)	7959 (−0.8 %)
2010	9137	8694 (−4.8 %)	NA	8950 (−2.0 %)

NA = not available

Table 2. Annual uncertainty estimates associated with CDIAC national emissions estimates. The uncertainty estimates were made following the method described by Andres et al. (2014). The national total emissions for the year 2013 were taken from Boden et al. (2016).

Ranking no.	Country	2013 emissions in kTC (% of the global total)	Uncertainty (%)
1	China	2 795 054 (28.6 %)	17.5
2	US	1 414 281 (14.5 %)	4.0
3	India	554 882 (5.7 %)	12.1
4	Russia Federation	487 885 (5.0 %)	14.8
5	Japan	339 074 (3.5 %)	4.0
6	Germany	206 521 (2.1 %)	4.0
7	Islamic Republic of Iran	168 251 (1.7 %)	9.4
8	Republic of Korea (South Korea)	161 576 (1.7 %)	12.1
9	Saudi Arabia	147 649 (1.5 %)	9.4
10	Brazil	137 354 (1.4 %)	12.1

gated, coarse spatial resolution. These issues will be further discussed in Sect. 7.

Because of the limitation mentioned above, here we compared emissions data only to characterize the differences that can be explained by the differences in emissions disaggregation methods. We implemented this comparison exercise using the 2008 emissions field aggregated at a $1 \times 1^\circ$ resolution. The year 2008 is the most recent year for which all the four emissions fields are available. The major emissions spatial patterns (e.g., emitting regions such as North America, Europe, and East Asia) are overall very similar as the correlations were driven by national emissions estimates (which we already saw to be in good agreement earlier), but we do see differences due to emissions disaggregation at the subnational level. Because of the use of nighttime light, ODIAC did not indicate emissions over some of the areas (e.g., Africa and Eurasia) while others are indicated. In particular, EDGAR shows emissions over those areas that are largely explained by line source emissions such as transportation. Overall, ODIAC tends to put more emissions towards populated areas than suburbs. This is also explained by the lack of line sources. In EDGAR v4.2, domestic fishery emissions can be seen, but not in EDGAR FT. Even in these two EDGAR versions, we can confirm the subnational differences in the United States, Europe, and China.

6.3 Regional emissions time series

Figure 8 shows time series of regional fossil fuel emissions aggregated over 11 land regions defined in the TransCom transport model intercomparison experiment (e.g., Gurney et al., 2002). The global seasonal variation and the associated uncertainty have been presented and discussed in Andres et al. (2011). Here monthly total emissions values were calculated for eleven TransCom land regions and presented with the associated uncertainty values (see Table 3). The monthly total values were calculated both excluding international bunker emissions (hence, land emissions only) and including the emissions. The uncertainty range was calculated with mass weighted uncertainty estimates of countries that fall into the TransCom regions. The uncertainty ranges shown in Fig. 8 show annual uncertainty plus the monthly profile uncertainty (12.8 %; reported by Andres et al., 2011). Monthly time series are presented for land-only emissions and land and international bunker emissions (here, largely aviation emissions). As described earlier, the emissions seasonality was adopted from Andres et al. (2011). The patterns in the emissions seasonality are often largely characterized by the large emitting countries within the regions (e.g., US for region 2 and China for region 8). Since Andres et al. (2011) used geographical closeness (also, type of economic systems) to define proxy countries, the countries in

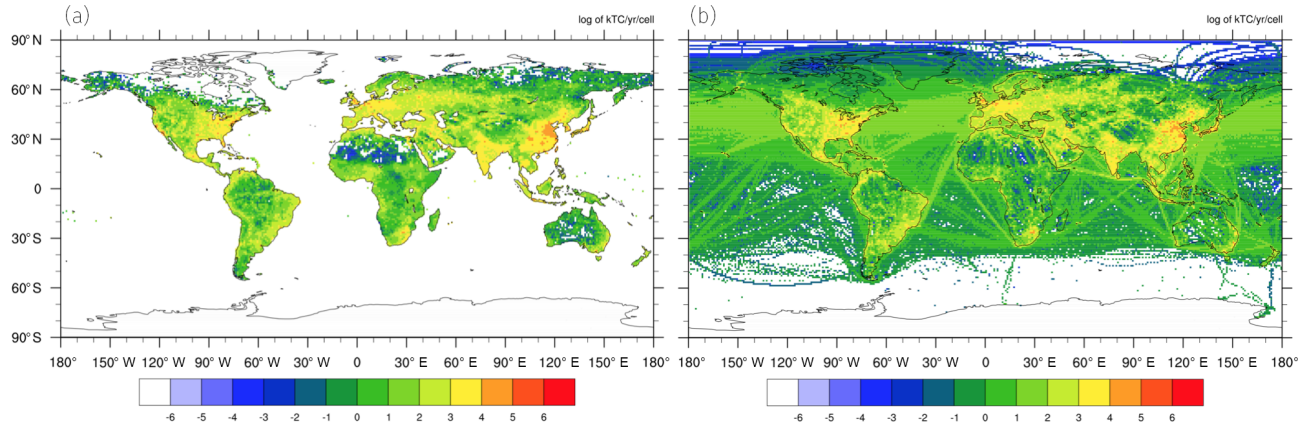

Figure 4. The 2013 global fossil fuel CO_2 emissions distributions from CDIAC (**a**, 8.36 PgC) and ODIAC (**b**, 9.78 PgC). The ODIAC emissions field was aggregated to a common $1 \times 1°$ resolution. The value is given in the unit of log of thousand tons C cell^{-1}.

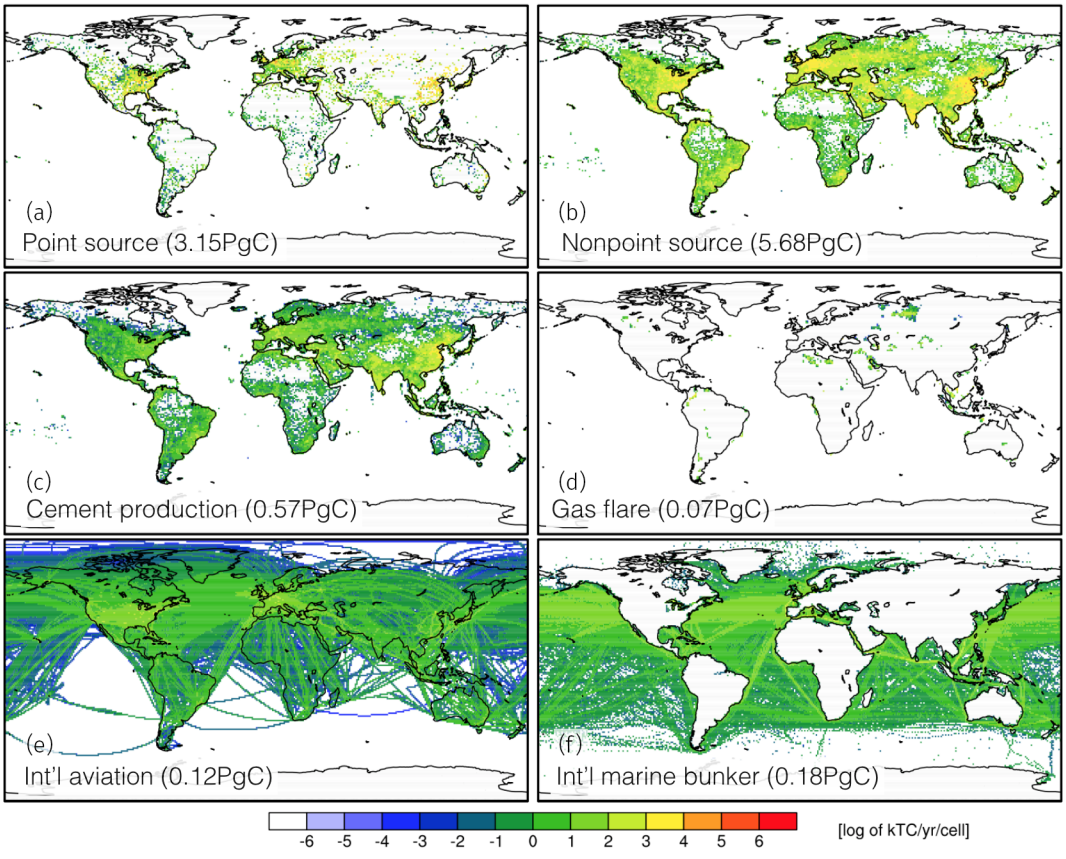

Figure 5. The 2013 global distributions of ODIAC fossil fuel emissions by emissions type. The panels show emissions from (from top to the right, then down) point source, nonpoint source, cement production, gas flaring, international aviation, and international shipping. The values in the figures are given in the unit of log of thousand tons of carbon per year per cell ($1 \times 1°$). The numbers in the brackets are the total for the category emissions in the unit of PgC (total 2013 emissions in ODIAC2016 was 9.78 PgC).

the same TransCom regions can have similar or the same seasonal patterns in their emissions.

As we can see in Fig. 4 (panel plot for aviation emissions), aviation emissions are intense over North America, Europe, and Asia. Global total aviation emissions was approximately 0.12 PgC yr^{-1} in 2013 and it often does not account for a large portion of the global total (1.2 % of the global total in 2013). However, considering the fact that those emissions are

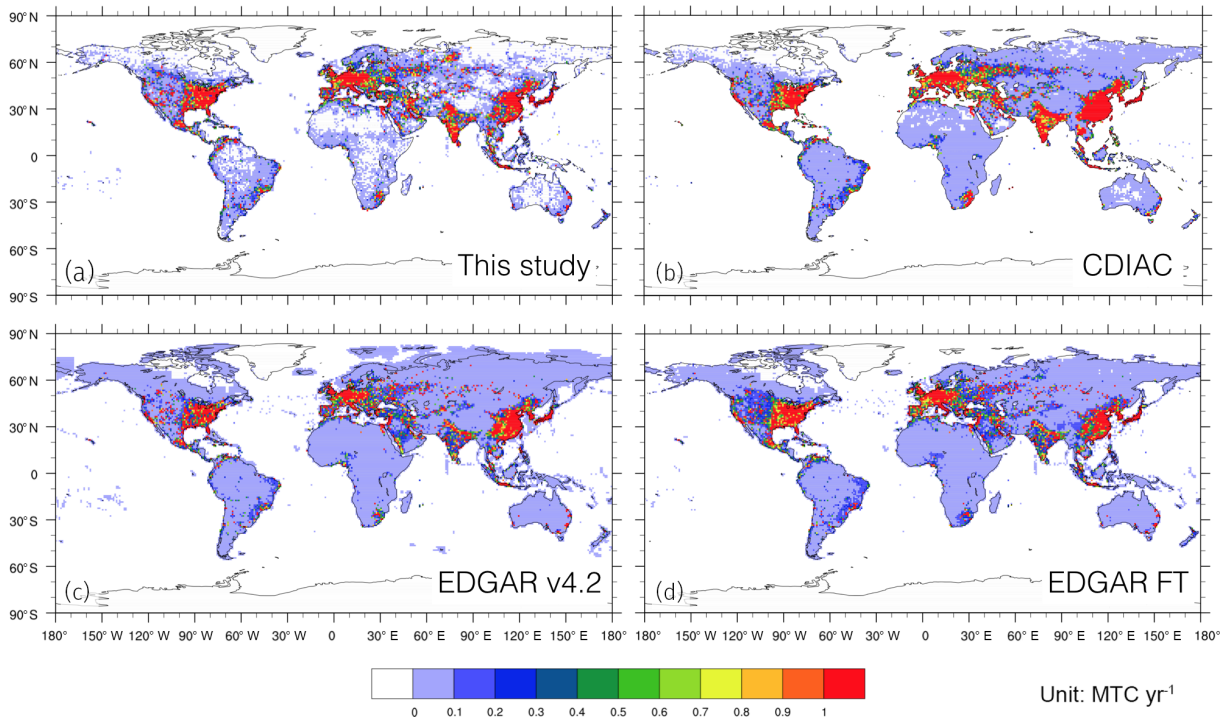

Figure 6. Land emissions from ODIAC **(a)**, CDIAC **(b)**, and two versions of EDGAR emissions data (v4.2, **c**; and v4.2 FastTrack, **d**). The units are million tons of carbon per year per cell ($1 \times 1°$). In addition to excluding emissions from international aviation and marine bunkers, some of the sector emissions were subtracted from EDGAR short cycle total emissions to account for the differences in emissions calculation methods between CDIAC and EDGAR. The emissions fields for the year 2008 were used.

concentrated in particular areas such as North America, Europe, and East Asia, rather than evenly distributed in space, and are often imposed at the surface layer in transport model simulation, care must be taken to achieve an accurate atmospheric CO_2 transport model simulation (Nassar et al., 2010). Aviation emissions were often around 0.5–5.1 % of the land total emissions over most regions, but also reached 12.7 % (North American Boreal).

7 Current limitations, caveats, and future prospects

As the ODIAC emissions data product is now used for a wide variety of carbon cycle research (e.g., global, regional inversions, urban emissions studies), it would be useful for the users of the ODIAC emissions data product to note and discuss issues, limitations, and caveats in our emissions data. Some of the issues and limitations are specific to our study; however, the majority of them are often shared by other existing gridded emissions data and emissions models.

7.1 Emissions estimates

In the production of ODIAC2016, we used several versions or editions of CDIAC estimates (e.g., global estimates, national estimates, and monthly gridded data). This could often happen in emissions data production, as some of the underlying data are not updated ro upgraded at the time of emissions data production (we often start updating emissions data after new fuel statistical data are released). We sometimes accept the inconsistency and try to use the most up-to-date information available. For example, we could use GCP's emissions estimates (e.g., Le Quéré et al., 2016) to constrain

Table 3. Annual uncertainty estimates over the TransCom land regions. The uncertainty estimates were mass weighted values of uncertainty estimates of countries that fall in the regions. Country uncertainty estimates were estimated using the method described (Andres et al., 2014). The values were reported as the 2σ uncertainty.

Region no.	Region name	Uncertainty (%)
1	North American Boreal	3.7
2	North American Temperate	3.7
3	South American Tropical	9.6
4	South American Temperate	12.8
5	Northern Africa	5.1
6	Southern Africa	10.6
7	Eurasian Boreal	12.4
8	Eurasian Temperate	7.8
9	Tropical Asia	11.8
10	Australia	4.0
11	Europe	3.8

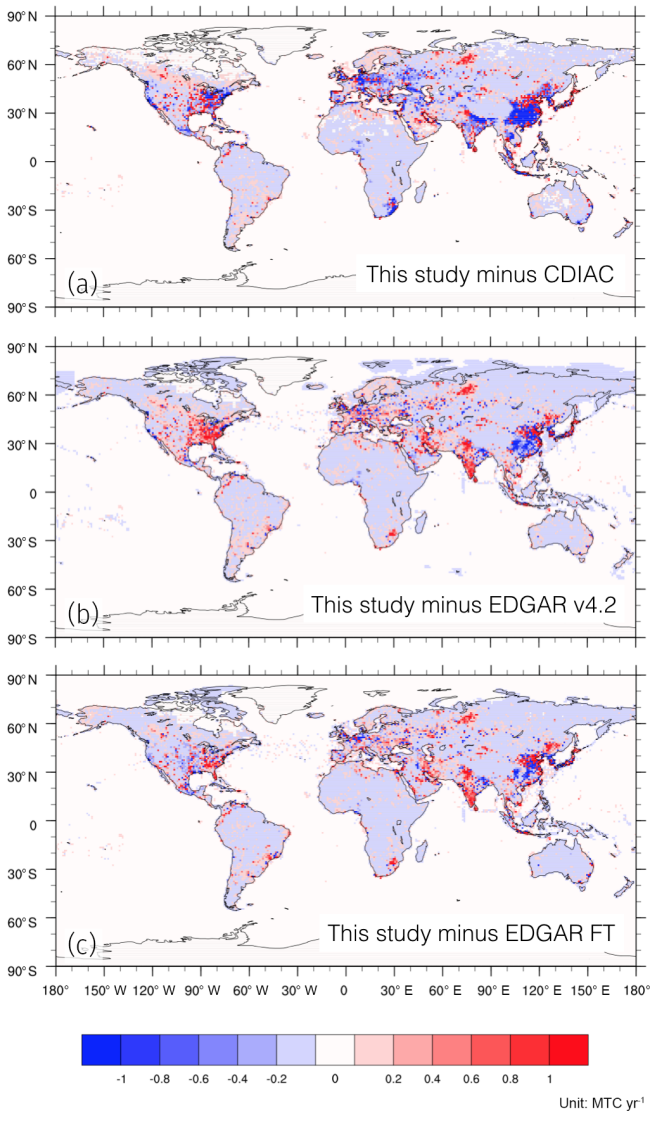

Figure 7. ODIAC minus other emissions data differences. CDIAC **(b)** and the two versions of EDGAR (v4.2, **c**; and v4.2 FastTrack, **d**). The units are million tons of carbon per year per cell ($1 \times 1°$). Note that the differences are defined as ODIAC (this study) minus others. The histograms of the differences are also presented in Fig. A1.

the global totals, if CDIAC global total emissions estimates are not available. The way we obtained emissions estimates for each version is often described in the NetCDF header information of the emissions data product. The use of the CARMA power plant estimates for estimating the magnitude of the point source portion of emissions is hard to eliminate, although ideally this is done using emissions estimates that are fully compatible with CDIAC estimates. We are currently examining UN statistical data (which CDIAC emissions estimates are based on) to assess the ability of explaining power plant emissions.

7.2 Emissions spatial distributions

7.2.1 Point source emissions

Although the use of the power plant geolocation allowed us to achieve improved high-resolution emissions spatial distributions over land (Oda and Maksyutov, 2011), the availability of power plant data is often very limited. For example, CARMA does not provide power plant emissions and their status (e.g., commission–decommission) every year. Furthermore, updates and upgrades after their version 3.0 database (which is dated to 2012) are also not provided. The error in their power plant geolocation is another issue that has been identified (e.g., Oda and Maksytuov, 2011; Woodard et al., 2015). In ODIAC, the base year emissions (2007) were projected and all the power plants were assumed to be active over the period (Oda and Maksyutov, 2011). There are only a few global projects such as the Global Energy Observatory (GEO, http://globalenergyobservatory.org/) that collect power plant information and those can be a useful source of data to improve and supplement the CARMA database. Regionally, CARMA can be evaluated using an inventory such as the US Emissions and Generation Resource Integrated Database (eGRID) (EPA, 2017). However, it is often difficult to find such a well-constructed and well-documented inventory for countries that are actually driving the uncertainty in global emissions (e.g., China and India).

Emissions from cement production (which are currently distributed by Ziskin et al., 2010, using nighttime light) and gas flare (which is distributed by Elvidge et al., 2009, using gas flare nighttime light data) should be distributed as point sources. For gas flare emissions, we examine the use of Nightfire (Elvidge at al., 2013a) to pinpoint active gas flares in a timely manner and improve their emissions spatial disaggregation over recent years. Currently, the point source emissions in ODIAC do not have an injection height due to the lack of global information. This limitation is shared with other existing global emissions data products.

7.2.2 Nonpoint source emissions

Nighttime light data have been an excellent proxy for human settlements (hence, CO_2 emissions) even at a high spatial resolution; however, there are some issues to be discussed. As mentioned earlier, we used an improved version of calibrated radiance data developed by Ziskin et al. (2010), but those data are only available for seven data periods over the course of the DMSP years (1992–2013). As we do not believe linearly interpolating the existing nighttime light data over the intervening years is necessarily the best way (as done in Asefi-Najafabady et al., 2014), the same nighttime light data have been used for some periods, and thus emissions distributions remain unchanged. We now examine the use of nighttime light data collected from the Visible Infrared Imaging Radiometer Suite (VIIRS) on the Suomi National Polar-orbiting Partnership satellite (e.g., Elvidge et al.,

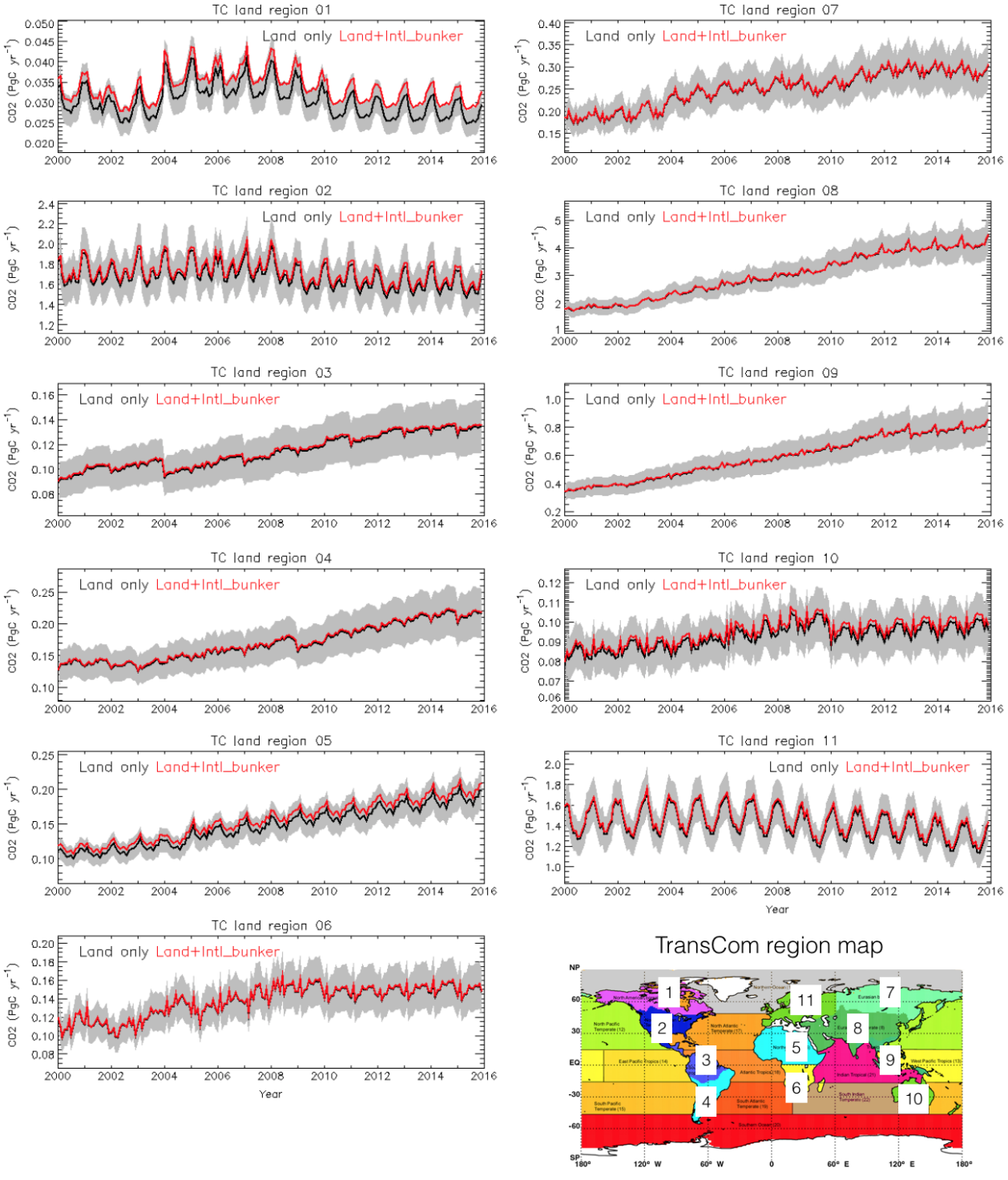

Figure 8. Emissions time series over inversion analysis land regions defined by the Transport Model Intercomparison Project (TransCom) (Gurney et al., 2002). The TransCom region map (bottom right) is available from http://transcom.project.asu.edu/transcom03_protocol_basisMap.php (last access: 8 November 2016). Black lines indicate the ODIAC $1 \times 1°$ monthly emissions. The monthly emissions are calculated using the $1 \times 1°$ ODIAC emissions data. The uncertainty range was calculated using mass weighted uncertainty estimates of countries that fall into the regions (see Table 3). The uncertainty ranges shown in this figure are annual uncertainty plus the monthly profile uncertainty (12.8 %; reported by Andres et al., 2011). Note that scales on the vertical axis are different.

2013b; Román and Stokes, 2015). VIIRS instruments do not have several of the critical issues that the DMSP instrument had (e.g., spatial resolution, dynamic range, quantization, and calibration) (Elvidge et al., 2013b). The fully calibrated nighttime light data can be used to map emissions changes in space in a timely and consistent manner.

In ODIAC, the disaggregation of nonpoint emissions is solely performed using nighttime light data for estimating subnational emissions spatial distributions, and no additional subnational emissions constraints were applied. Rayner et al. (2010) proposed to better constrain subnational emissions spatial distribution by combining population data, nighttime lights, and GDP in their Fossil Fuel Data Assimilation System (FFDAS) framework. Asefi-Najafabady et al. (2014) further introduced the use of point source information in their disaggregation; the optimization in their current framework is however under-constrained by the lack of GDP information. Without having such optimization, the state level per capita emissions estimates can provide subnational constraints. Nassar et al. (2013) evaluated the per capita emissions in CDIAC and ODIAC emissions data over Canada using the national inventory and found that ODIAC outperformed. However, as the nighttime light–population relationship might have a bias for developing and the least developed countries (Raupach et al., 2010), we would expect to see significant biases over those countries and the per capita estimates can provide a useful constraint.

As seen in the comparison to other emissions data, the major difference from EDGAR emissions spatial distribution was due to the lack of line sources in ODIAC. We do not believe the result from the emissions data comparison can falsify the emissions distribution in ODIAC, as discussed earlier. However, we do expect an inclusion of the line sources would improve the spatial distributions and emissions representations in both cities and rural areas. We are currently examining the inclusion of transportation network data (e.g., OpenStreetMap) as a proxy for line source emissions to explore the better spatial emissions aggregation method. Oda et al. (2017) recently implemented the idea of adding a spatial proxy for line sources and improved emissions estimates for a US city.

7.2.3 Aviation emissions

We estimated emissions from international aviation from CDIAC using UN statistical data. The emissions are currently provided as a single layer emissions field, although this is not appropriate given the nature of the aviation emissions. Nassar et al. (2010) discussed the importance of the three-dimensional (e.g., x, y, z) emissions for interpreting the CO_2 profile. In the current modeling framework, although we maintain the aviation emissions injection height from AERO2k (reduced to 1 km interval), we distribute the emissions to a single layer. As pointed out by Olsen et al. (2013), AERO2k does not agree with other inventories in height distribution. While noting this inconsistency, we will examine the use of height information from AERO2k and other data available to us and do sensitivity analysis using transport model simulations.

7.3 Emissions temporal profiles

The emissions seasonality in ODIAC2016 is based on Andres et al. (2011) and it can be further extended to an hourly scale using the TIMES scaling parameter. We note that the emissions seasonality was based on the top 10 emitting countries' fuel statistics and Monte Carlo simulation (Andres et al., 2011). The emissions seasonality for countries other than the top 10 could be less robust. Also, because of the use of Monte Carlo, the seasonality is different over different editions of monthly emissions data. It is also important to note that the repeated use of climatological (mean) seasonality for recent years (described in Sect. 5) could be a source of uncertainty and bias. Andres et al. (2011) estimated the monthly uncertainty as 12.8 % (2σ) in addition to the annual emissions uncertainty. As we often impose fossil fuel emissions, care must be taken when applied to inversions. Ultimately, as carried out by Vogel et al. (2013), we might be able to evaluate temporal profiles from statistical data and improve them (but only to limited small locations).

7.4 Uncertainties associated with gridded emissions fields

As mentioned earlier, the evaluation of gridded emissions data is often very challenging and most of the emissions data studies share this difficulty. Although the emissions estimates are made on global and national scales with small uncertainties (e.g., 8 % for the global scale by Andres et al., 2014), considerable errors seem to be introduced when the emissions are disaggregated (e.g., Hogue et al., 2016; Andres et al., 2016). Andres et al. (2016), for example, estimated the uncertainty associated with CDIAC gridded emissions data on a per grid cell basis with an average of 120 % and a range of 4.0 to 190 % (2σ). Hogue et al. (2016) looked closely at CDIAC gridded emissions data over the US domain and estimated the uncertainty associated with the $1 \times 1^\circ$ emissions grids as ± 150 %. Those errors seem to be unique to the disaggregation method (Andres et al., 2016). Future funding may allow us to pursue a full uncertainty analysis of the ODIAC emissions data and model, akin to the Andres et al. (2016) approach but accounting for the greater-than-one carbon distribution mechanisms utilized in the ODIAC emissions modeling framework. All of the spatially distributed gridded emissions data mentioned in this paper suffer from the same basic defect: they use proxies to spatially distribute emissions rather than actual measurements. In addition, evaluating emissions distributions based on a nighttime light proxy can be challenging as the connection between CO_2 emissions and proxy is less direct compared to population (e.g., per

capita emissions). A combined use of emissions proxy and geolocation data (e.g., power plant location) would also add additional difficulties to finding a comprehensive measure of the uncertainty because of different types of error and uncertainty sources (e.g., Woodard et al., 2015). As finer spatial scales are approached, the defect of the proxy approach becomes more apparent: proxies only estimate emissions fields. The ODIAC data product has been used not only for global simulations at an aggregated spatial resolution, but also at very high spatial resolution (e.g., Ganshin et al., 2012; Oda et al., 2012, 2017; Lauvaux et al., 2016). Thus, an emissions evaluation at a high resolution has become an important task. One approach we could take for evaluating high-resolution emissions fields is comparing to a local finely grained emissions data product such as Gurney et al. (2012), acknowledging the limitations of the approach discussed earlier. Another approach would be evaluating emissions data in concentration space rather than emissions space. As reported in Vogel et al. (2013) and Lauvaux et al. (2016), with radiocarbon measurements and/or good, spatially dense CO_2 measurements, a high-resolution transport model simulation can provide an objective measure for emissions data evaluations (e.g., model–observation mismatch and emissions inverse estimate).

While the quality (i.e., bias and uncertainty) of the gridded emissions estimates remains unquantified for most of the emissions data mentioned in this paper, the emissions data are still used because sufficient measurements in space and time are not presently available to offer a better alternative. At the very least, we presented the uncertainty estimates over the aggregated TransCom land regions. We believe that the regional uncertainty estimates are highly useful for atmospheric CO_2 inversion modelers, more than uncertainty estimates at a grid level, which still do not seem to be ready for use. Inversion studies often aggregate flux estimates over the TransCom land regions to interpret regional carbon budgets, while flux estimations in their models are performed at much higher spatial resolutions (e.g., Feng et al., 2009; Chevallier et al., 2010; Basu et al., 2013). Taking advantage of the ODIAC emissions dataset being based on the CDIAC estimates, we adopted the updated uncertainty estimates reported by Andres et al. (2016) and obtained the regional uncertainty estimates. Those estimates are new and readily usable for the inversion studies, especially when interpreting the regional estimates.

8 Product distribution, data policy, and future update

The ODIAC2016 data product is available from a website hosted by the Center for Global Environmental Research (CGER), Japanese National Institute for Environmental Studies (NIES) (http://db.cger.nies.go.jp/dataset/ODIAC/, https://doi.org/10.17595/20170411.001). The data product is distributed under Creative Commons Attribution 4.0 International (CC-BY 4.0, https://creativecommons.org/licenses/by/4.0/deed.en). The ODIAC2016 emissions data are provided in two file formats: (1) a global 1×1 km (30 arcsec) monthly file in the GeoTIFF format (only includes emissions over land) and (2) a $1 \times 1^\circ$ annual (12 month) file in the NetCDF format (includes international bunker emissions). A single, global 1×1 km monthly GeoTIFF file is about 3.7 GB (compressed to 120 MB). A $1 \times 1^\circ$ single NetCDF annual file is about 6 MB.

We update the emissions data on an annual basis, following the release of an updated global fuel statistical data. Future versions of the emissions data are in principle based on an updated version or edition of the underlying statistical data with the same name convention (ODIACYYYY, YYYY is the release year; the end year is YYYY minus 1). In October 2017, we started distributing the updated 2017 version of ODIAC data (ODIAC2017, 2000–2016). We primarily focus on years after 2000. Future versions of ODIAC data, however, might have a longer, extended time coverage.

9 Data availability

For detailed information about data availability, please refer to Sect. 8 in this paper.

10 Summary

This paper describes the 2016 version of ODIAC emissions data (ODIAC2016) and how the emissions data product was developed within our upgraded emissions modeling framework. Based on the CDIAC emissions data, ODIAC2016 can be viewed as an extended version of the CDIAC gridded data with improved emissions spatial distribution representations. Utilizing the best available data (emissions estimates and proxy), we achieved a comprehensive, global fossil fuel CO_2 gridded emissions field that allows data users to impose their CO_2 simulations in a consistent way with many of the global carbon budget analyses. With updated fuel statistics, we should be able to continue producing updated future versions of the ODIAC emissions data product within the same model framework. The capability we developed in this study has become more significant now, given the CDIAC/ORNL's shutdown. Despite expected difficulties (e.g., discontinued CDIAC estimates), the authors believe that ODIAC could play an important role in delivering emissions data to the carbon cycle science community. Limitations and caveats discussed in this paper mirror and lead ODIAC's future prospects. The ODIAC emissions data product is distributed from http://db.cger.nies.go.jp/dataset/ODIAC/ with a DOI. Currently the 2017 version of ODIAC emissions data (ODIAC2017, 2000–2016) is also available.

Appendix A

Table A1. A list of components in ODIAC2016 and data used in the development.

Component	Data/product name	Description and data source	Reference
Global FFCO2	CDIAC global fossil fuel CO_2 emissions	The 2016 edition of the CDIAC global total estimates was used to constrain the ODIAC2016 totals. Data are available at http://cdiac.ornl.gov/ftp/ndp030/global.1751_2013.ems.	Boden et al. (2016)
National FFCO2	CDIAC fossil fuel CO_2 emissions by Nation	The 2016 editions of the CDIAC national emissions estimates are used as primary input data. Data are available at http://cdiac.ornl.gov/ftp/ndp030/nation.1751_2013.ems.	Boden et al. (2016)
Global fuel statistics	BP statistical review of world energy	The 2016 edition of the BP statistical data was used to project CDIAC national emissions over recent years (2014–2015). Data are available at http://www.bp.com/en/global/corporate/energy-economics/statistical-review-of-world-energy.html.	BP (2017)
Monthly temporal variation	CDIAC gridded monthly estimate	The 2013 version of the CDIAC monthly gridded data was used to the model seasonality in ODIAC2016. Data are available at http://cdiac.ornl.gov/ftp/fossil_fuel_CO2_emissions_gridded_monthly_v2013/.	Andres et al. (2011)
Power plant data	CARMA	The CARMA power plant database with geolocation correction described in Oda and Maksyutov (2011). Data are available from http://carma.org/.	Wheeler and Ummel (2008)
NTL (for nonpoint emissions)	Global radiance calibrated nighttime lights	Multiple-year NTL data are used to distribute nonpoint emissions. Data are available at https://ngdc.noaa.gov/eog/dmsp/download_radcal.html.	Ziskin et al. (2010)
NTL (for gas flaring)	Global gas flaring shapefiles	Global gas flaring NTL data are specifically used to distribute gas flaring emissions. Data are available at http://ngdc.noaa.gov/eog/interest/gas_flares_countries_shapefiles.html.	Elvidge et al. (2009)
Int'l ship tracks	EDGAR v4.1	The international marine bunker emissions field in EDGAR v4.1 was used. Data are available at http://edgar.jrc.ec.europa.eu/archived_datasets.php.	JRC (2017)
Int'l aviation flight tracks	AERO2k	Data were used to distribute aviation emissions. More details can be found at http://www.cate.mmu.ac.uk/projects/aero2k/.	Eyers et al. (2005)
Weekly and diurnal cycle	TIMES	This was not a part of ODIAC2016; however, it is useful to note that these scaling factors can be used to create weekly and diurnally varying emissions. Data are available at http://cdiac.ornl.gov/ftp/Nassar_Emissions_Scale_Factors/.	Nassar et al. (2013)

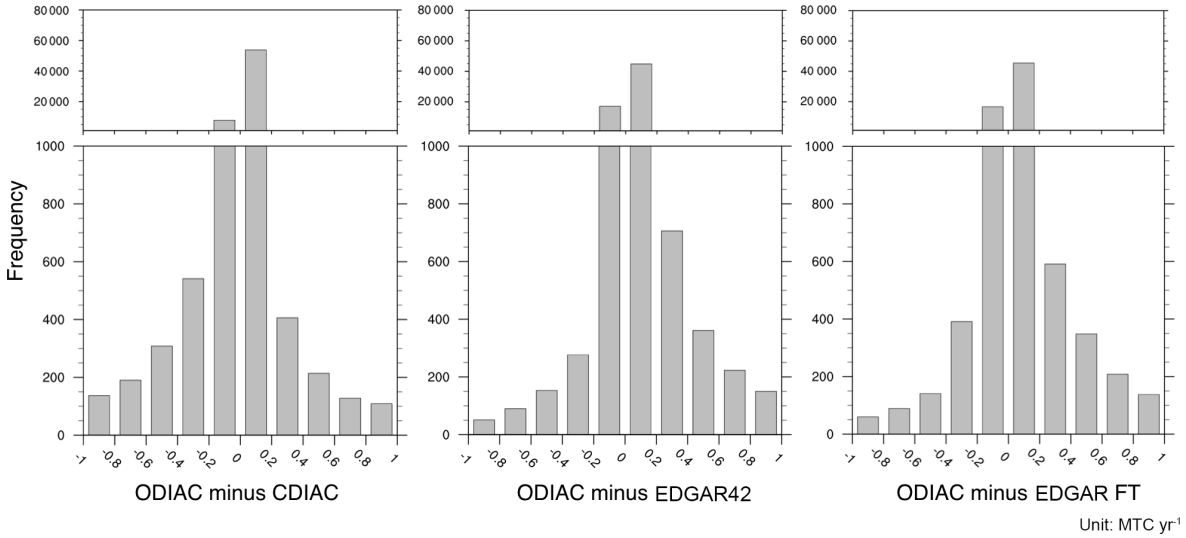

Figure A1. A histogram of the inter-emissions data differences from ODIAC. Values are given in the unit of million tons carbon per year (MTC yr^{-1}).

Table A2. A table for the global scaling factor for 2000–2013.

Year	Scaling factor
2000	0.999
2001	1.016
2002	1.008
2003	1.014
2004	1.012
2005	1.022
2006	1.022
2007	1.016
2008	1.023
2009	1.024
2010	1.015
2011	1.017
2012	1.017
2013	1.025

Competing interests. The authors declare that they have no conflict of interest.

Acknowledgements. Tomohiro Oda is supported by the NASA Carbon Cycle Science program (grant no. NNX14AM76G). RJA is now retired but this work was sponsored by US Department of Energy, Office of Science, Biological and Environmental Research (BER) programs and performed at the Oak Ridge National Laboratory (ORNL) under the US Department of Energy contract DE-AC05-00OR22725. The authors would like to thank Chris Elvidge and Kim Baugh at NOAA/NGDC for providing the nighttime light data. The authors also thank Yasuhiro Tsukada and Tomoko Shirai for hosting the ODIAC emissions data on the data server at NIES.

Edited by: David Carlson
Reviewed by: two anonymous referees

References

Andres, R. J., Marland, G., Fung, I., and Matthews, E.: A $1° \times 1°$ distribution of carbon dioxide emissions from fossil fuel consumption and cement manufacture, 1950–1990, Global Biogeochem. Cy., 10, 419–429, https://doi.org/10.1029/96GB01523, 1996.

Andres R. J., Gregg J. S., Losey, L., Marland, G., and Boden, T. A.: Monthly, global emissions of carbon dioxide from fossil fuel consumption, Tellus B, 63, 309-0327, https://doi.org/10.1111/j.1600-0889.2011.00530.x, 2011.

Andres, R. J., Boden, T. A., Bréon, F.-M., Ciais, P., Davis, S., Erickson, D., Gregg, J. S., Jacobson, A., Marland, G., Miller, J., Oda, T., Olivier, J. G. J., Raupach, M. R., Rayner, P., and Treanton, K.: A synthesis of carbon dioxide emissions from fossil-fuel combustion, Biogeosciences, 9, 1845–1871, https://doi.org/10.5194/bg-9-1845-2012, 2012.

Andres, R. J., Boden, T. A., and Higdon, D.: A new evaluation of the uncertainty associated with CDIAC estimates of fossil fuel carbon dioxide emission, Tellus B, 66, 23616, https://doi.org/10.3402/tellusb.v66.23616, 2014.

Andres, R. J., Boden, T. A., and Higdon, D. M.: Gridded uncertainty in fossil fuel carbon dioxide emission maps, a CDIAC example, Atmos. Chem. Phys., 16, 14979–14995, https://doi.org/10.5194/acp-16-14979-2016, 2016.

Asefi-Najafabady, S., Rayner, P. J., Gurney, K. R., McRobert, A., Song, Y., Coltin, K., Huang, J., Elvidge, C., and Baugh, K.: A multiyear, global gridded fossil fuel CO_2 emission data product: Evaluation and analysis of results, J. Geophys. Res.-Atmos., 119, 10213–10231, https://doi.org/10.1002/2013JD021296, 2014.

Baker, D. F., Doney, S. C., and Schimel, D. S.: Variational data assimilation for atmospheric CO_2, Tellus B, 58, 359–365, https://doi.org/10.1111/j.1600-0889.2006.00218.x, 2006.

Ballantyne, A. P., Alden, C. B., Miller, J. B., Tans, P. P., and White, J. W. C.: Increase in observed net carbon dioxide uptake by land and oceans during the past 50 years, Nature, 488, 70–72, 2012.

Basu, S., Guerlet, S., Butz, A., Houweling, S., Hasekamp, O., Aben, I., Krummel, P., Steele, P., Langenfelds, R., Torn, M., Biraud, S., Stephens, B., Andrews, A., and Worthy, D.: Global CO_2 fluxes estimated from GOSAT retrievals of total column CO_2, Atmos. Chem. Phys., 13, 8695–8717, https://doi.org/10.5194/acp-13-8695-2013, 2013.

Boden, T. A., Marland, G., and Andres, R. J.: Global, Regional, and National Fossil-Fuel CO_2 Emissions, Carbon Dioxide Information Analysis Center, Oak Ridge National Laboratory, U.S. Department of Energy, Oak Ridge, Tenn., USA, https://doi.org/10.3334/CDIAC/00001_V2016, 2016.

Boden, T. A., Marland, G., and Andres, R. J.: Global, Regional, and National Fossil-Fuel CO_2 Emissions, Carbon Dioxide Information Analysis Center, Oak Ridge National Laboratory, U.S. Department of Energy, Oak Ridge, Tenn., USA, https://doi.org/10.3334/CDIAC/00001_V2017, 2017.

Bousquet, P., Ciais, P., Peylin, P., Ramonet, M., and Monfray, P.: Inverse modeling of annual atmospheric CO_2 sources and sinks 1. Method and control inversion, J. Geophys. Res., 104, 26161–26178, 1999.

BP: Statistical Review of World Energy, available at: http://www.bp.com/en/global/corporate/energy-economics/statistical-review-of-world-energy.html, last access: 6 June 2017.

Brioude, J., Angevine, W. M., Ahmadov, R., Kim, S.-W., Evan, S., McKeen, S. A., Hsie, E.-Y., Frost, G. J., Neuman, J. A., Pollack, I. B., Peischl, J., Ryerson, T. B., Holloway, J., Brown, S. S., Nowak, J. B., Roberts, J. M., Wofsy, S. C., Santoni, G. W., Oda, T., and Trainer, M.: Top-down estimate of surface flux in the Los Angeles Basin using a mesoscale inverse modeling technique: assessing anthropogenic emissions of CO, NO_x and CO_2 and their impacts, Atmos. Chem. Phys., 13, 3661–3677, https://doi.org/10.5194/acp-13-3661-2013, 2013.

Chevallier, F., Ciais, P., Conway, T. J., Aalto, T., Anderson, B. E., Bousquet, P., Brunke, E. G., Ciattaglia, L., Esaki, Y., Fröhlich, M., Gomez, A., Gomez-Pelaez, A. J., Haszpra, L., Krummel, P. B., Langenfelds, R. L., Leuenberger, M., Machida, T., Maignan, F., Matsueda, H., Morgué, J. A., Mukai, H., Nakazawa, T., Peylin, P., Ramonet, M., Rivier, L., Sawa, Y., Schmidt, M., Steele, L. P., Vay, S. A., Vermeulen, A. T., Wofsy, S., Worthy, D.: CO_2 surface fluxes at grid point scale estimated from a global 21 year reanalysis of atmospheric measurements, J. Geophys. Res., 115, D21307, https://doi.org/10.1029/2010JD013887, 2010.

Doll, C. N. H., Muller, J.-P., and Elvidge, C. D.: Nighttime imagery as a tool for global mapping of socioeconomic parameters and greenhouse gas emissions, Ambio, 29, 157–162, 2000.

Elvidge, C. D., Baugh, K. E., Dietz, J. B., Bland, T., Sutton, P. C., and Kroehl, H. W.: Radiance calibration of DMSP-OLS lowLight imaging data of human settlements – a new device for portraying the Earth's surface entire, Remote Sens. Environ., 68, 77–88, 1999.

Elvidge, C. D., Ziskin, D., Baugh, K. E., Tuttle, B. T., Ghosh, T., Pack, D. W., Erwin, E. H., and Zhizhin, M.: A Fifteen Year Record of Global Natural Gas Flaring Derived from Satellite Data, Energies, 2, 595–622, 2009.

Elvidge, C. D., Zhizhin, M., Hsu, F.-C., and Baugh, K. E.: VIIRS Nightfire: Satellite pyrometry at night, Remote Sensing, 5, 4423–4449, 2013a.

Elvidge, C. D., Baugh, K. E., Zhizhin, M., and Hsu, F.-C.: Why VIIRS data are superior to DMSP for mapping nighttime lights, Proceedings of the Asia-Pacific Advanced Network, 35, 62–69, https://doi.org/10.7125/apan.35.7, 2013b.

EPA: Emissions and Generation Resource Integrated Database (eGRID), available at: https://www.epa.gov/energy/emissions-generation-resource-integrated-database-egrid, last access: 6 June 2017.

Eyers, C. J., Norman, P., Middel, J., Plohr, M., Michot, S., Atkinson, K., and Christou, R. A.: AERO2k Global Aviation Emissions Inventories for 2002 and 2025, QinetiQ/04/001113, 2005.

Feng, L., Palmer, P. I., Bösch, H., and Dance, S.: Estimating surface CO_2 fluxes from space-borne CO_2 dry air mole fraction observations using an ensemble Kalman Filter, Atmos. Chem. Phys., 9, 2619–2633, https://doi.org/10.5194/acp-9-2619-2009, 2009.

Feng, L., Palmer, P. I., Parker, R. J., Deutscher, N. M., Feist, D. G., Kivi, R., Morino, I., and Sussmann, R.: Estimates of European uptake of CO_2 inferred from GOSAT X_{CO_2} retrievals: sensitivity to measurement bias inside and outside Europe, Atmos. Chem. Phys., 16, 1289–1302, https://doi.org/10.5194/acp-16-1289-2016, 2016.

Feng, L., Palmer, P. I., Bösch, H., Parker, R. J., Webb, A. J., Correia, C. S. C., Deutscher, N. M., Domingues, L. G., Feist, D. G., Gatti, L. V., Gloor, E., Hase, F., Kivi, R., Liu, Y., Miller, J. B., Morino, I., Sussmann, R., Strong, K., Uchino, O., Wang, J., and Zahn, A.: Consistent regional fluxes of CH_4 and CO_2 inferred from GOSAT proxy XCH_4:XCO_2 retrievals, 2010–2014, Atmos. Chem. Phys., 17, 4781–4797, https://doi.org/10.5194/acp-17-4781-2017, 2017.

Feng, S., Lauvaux, T., Newman, S., Rao, P., Ahmadov, R., Deng, A., Díaz-Isaac, L. I., Duren, R. M., Fischer, M. L., Gerbig, C., Gurney, K. R., Huang, J., Jeong, S., Li, Z., Miller, C. E., O'Keeffe, D., Patarasuk, R., Sander, S. P., Song, Y., Wong, K. W., and Yung, Y. L.: Los Angeles megacity: a high-resolution land–atmosphere modelling system for urban CO_2 emissions, Atmos. Chem. Phys., 16, 9019–9045, https://doi.org/10.5194/acp-16-9019-2016, 2016.

Ganshin, A., Oda, T., Saito, M., Maksyutov, S., Valsala, V., Andres, R. J., Fisher, R. E., Lowry, D., Lukyanov, A., Matsueda, H., Nisbet, E. G., Rigby, M., Sawa, Y., Toumi, R., Tsuboi, K., Varlagin, A., and Zhuravlev, R.: A global coupled Eulerian-Lagrangian model and 1×1 km CO_2 surface flux dataset for high-resolution atmospheric CO_2 transport simulations, Geosci. Model Dev., 5, 231–243, https://doi.org/10.5194/gmd-5-231-2012, 2012.

Ghosh, T., Elvidge, C. D., Sutton, P. C., Baugh, K. E., Ziskin, D., and Tuttle, B. T.: Creating a Global Grid of Distributed Fossil Fuel CO_2 Emissions from Nighttime Satellite Imagery, Energies, 3, 1895–1913, 2010.

Gurney, K. R., Law, R. M., Denning, A. S., Rayner, P. J., Baker, D., Bousquet, P., Bruhwiler, L., Chen, Y. H., Ciais, P., Fan, S., Fung, I. Y., Gloor, M., Heimann, M., Higuchi, K., John, J., Maki, T., Maksyutov, S., Masarie, K., Peylin, P., Prather, M., Pak, B. C., Randerson, J., Sarmiento, J., Taguchi, S., Takahashi, T., and Yuen, C. W.: Towards robust regional estimates of CO_2 sources and sinks using atmospheric transport models, Nature, 415, 626–630, 2002.

Gurney, K. R., Chen, Y.-H., Maki, T., Kawa, S. R., Andrews, A., and Zhu, Z.: Sensitivity of atmospheric CO_2 inversions to seasonal and interannual variations in fossil fuel emissions, J. Geophys. Res., 110, D10308, https://doi.org/10.1029/2004JD005373, 2005.

Gurney, K. R., Mendoza, D., Zhou, Y., Fischer, M., de la Rue du Can, S., Geethakumar, S., and Miller, C.: The Vulcan Project: High resolution fossil fuel combustion CO_2 emissions fluxes for the United States, Environ. Sci. Technol., 43, https://doi.org/10.1021/es900806c, 2009.

Gurney, K., Razlivanov, I., Song, Y., Zhou, Y., Benes, B., and Abdul-Massih, M.: Quantification of fossil fuel CO_2 emission on the building/street scale for a large US city, Environ. Sci. Technol., 46, 12194–12202, 2012.

Hakkarainen, J., Ialongo, I., and Tamminen, J.: Direct space-based observations of anthropogenic CO_2 emission areas from OCO-2, Geophys. Res. Lett., 43, 11400–11406, https://doi.org/10.1002/2016GL070885, 2016.

Hogue, S., Marland, E., Andres, R. J., Marland, G., and Woodard, D.: Uncertainty in gridded CO_2 emissions estimates, Earth's Future, 4, 225–239, https://doi.org/10.1002/2015EF000343, 2016.

Hutchins, M. G., Colby, J. D., Marland, G., and Marland, E.: A comparison of five high-resolution spatially-explicit, fossil-fuel, carbon dioxide emission inventories for the United States, Mitig. Adapt. Strat. Gl., 22, 947–972, https://doi.org/10.1007/s11027-016-9709-9, 2016.

Janardanan, R., Maksyutov, S., Oda, T., Saito, M., Kaiser, J. W., Ganshin, A., Stohl, A., Matsunaga, T., Yoshida, Y., and Yokota, T.: Comparing GOSAT observations of localized CO_2 enhancements by large emitters with inventory-based estimates, Geophys. Res. Lett., 43, 3486–3493, https://doi.org/10.1002/2016GL067843, 2016.

Janssens-Maenhout, G., Dentener, F., Van Aardenne, J., Monni, S., Pagliari, V., Orlandini, L., Klimont, Z., Kurokawa, J., Akimoto, H., Ohara, T., Wankmueller, R., Battye, B., Grano, D., Zuber, A., and Keating, T.: EDGAR-HTAP: a Harmonized Gridded Air Pollution Emission Dataset Based on National Inventories, Ispra (Italy): European Commission Publications Office, 2012, JRC68434, EUR report No EUR 25 299 - 2012, ISBN 978-92-79-23122-0, ISSN 1831-9424, 2012.

JRC: EDGAR – Emissions Database for Global Atmospheric Research, available at: http://edgar.jrc.ec.europa.eu/, last access: June 2017.

Kurokawa, J., Ohara, T., Morikawa, T., Hanayama, S., Janssens-Maenhout, G., Fukui, T., Kawashima, K., and Akimoto, H.: Emissions of air pollutants and greenhouse gases over Asian regions during 2000–2008: Regional Emission inventory in ASia (REAS) version 2, Atmos. Chem. Phys., 13, 11019–11058, https://doi.org/10.5194/acp-13-11019-2013, 2013.

Lauvaux, T., Miles, N. L., Deng, A., Richardson, S. J., Cambaliza, M. O., Davis, K. J., Gaudet, B., Gurney, K. R., Huang, J., O'Keefe, D., Song, Y., Karion, A., Oda, T., Patarasuk, R., Razlivanov, I., Sarmiento, D., Shepson, P., Sweeney, C., Turnbull, J., and Wu, K.: High-resolution atmospheric inversion of urban CO_2 emissions during the dormant season of the Indianapolis Flux Experiment (INFLUX), J. Geophys. Res.-Atmos., 121, 5213–5236, https://doi.org/10.1002/2015JD024473, 2016.

Le Quéré, C., Andrew, R. M., Canadell, J. G., Sitch, S., Korsbakken, J. I., Peters, G. P., Manning, A. C., Boden, T. A., Tans, P. P., Houghton, R. A., Keeling, R. F., Alin, S., Andrews, O. D., Anthoni, P., Barbero, L., Bopp, L., Chevallier, F., Chini, L. P., Ciais, P., Currie, K., Delire, C., Doney, S. C., Friedlingstein, P., Gkritzalis, T., Harris, I., Hauck, J., Haverd, V., Hoppema, M., Klein Goldewijk, K., Jain, A. K., Kato, E., Körtzinger, A., Landschützer, P., Lefèvre, N., Lenton, A., Lienert, S., Lombardozzi, D., Melton, J. R., Metzl, N., Millero, F., Monteiro, P. M. S.,

Munro, D. R., Nabel, J. E. M. S., Nakaoka, S.-I., O'Brien, K., Olsen, A., Omar, A. M., Ono, T., Pierrot, D., Poulter, B., Rödenbeck, C., Salisbury, J., Schuster, U., Schwinger, J., Séférian, R., Skjelvan, I., Stocker, B. D., Sutton, A. J., Takahashi, T., Tian, H., Tilbrook, B., van der Laan-Luijkx, I. T., van der Werf, G. R., Viovy, N., Walker, A. P., Wiltshire, A. J., and Zaehle, S.: Global Carbon Budget 2016, Earth Syst. Sci. Data, 8, 605–649, https://doi.org/10.5194/essd-8-605-2016, 2016.

Maksyutov, S., Takagi, H., Valsala, V. K., Saito, M., Oda, T., Saeki, T., Belikov, D. A., Saito, R., Ito, A., Yoshida, Y., Morino, I., Uchino, O., Andres, R. J., and Yokota, T.: Regional CO_2 flux estimates for 2009–2010 based on GOSAT and ground-based CO_2 observations, Atmos. Chem. Phys., 13, 9351–9373, https://doi.org/10.5194/acp-13-9351-2013, 2013.

Marland, G. and Rotty, R. M.: Carbon dioxide emissions from fossil fuels: a procedure for estimation and results for 1950–1982, Tellus B, 36B, 232–261, https://doi.org/10.1111/j.1600-0889.1984.tb00245.x, 1984.

Myhre, G., Alterskjær, K., and Lowe, D.: A fast method for updating global fossil fuel carbon dioxide emissions, Environ. Res. Lett., 4, 034012, https://doi.org/10.1088/1748-9326/4/3/034012, 2009.

Nassar, R., Jones, D. B. A., Suntharalingam, P., Chen, J. M., Andres, R. J., Wecht, K. J., Yantosca, R. M., Kulawik, S. S., Bowman, K. W., Worden, J. R., Machida, T., and Matsueda, H.: Modeling global atmospheric CO_2 with improved emission inventories and CO_2 production from the oxidation of other carbon species, Geosci. Model Dev., 3, 689–716, https://doi.org/10.5194/gmd-3-689-2010, 2010.

Nassar, R., Napier-Linton, L., Gurney, K. R., Andres, R. J., Oda, T., Vogel, F. R., and Deng, F.: Improving the temporal and spatial distribution of CO_2 emissions from global fossil fuel emission data sets, J. Geophys. Res.-Atmos., 118, 917–933, https://doi.org/10.1029/2012JD018196, 2013.

Oda, T. and Maksyutov, S.: A very high-resolution (1 km × 1 km) global fossil fuel CO_2 emission inventory derived using a point source database and satellite observations of nighttime lights, Atmos. Chem. Phys., 11, 543–556, https://doi.org/10.5194/acp-11-543-2011, 2011.

Oda, T. and Maksyutov, S.: Open-source Data Inventory for Anthropogenic CO_2 (ODIAC) emission dataset, National Institute for Environmental Studies, Tsukuba, Japan, https://doi.org/10.17595/20170411.001, available at: http://db.cger.nies.go.jp/dataset/ODIAC/ (last access: 10 January 2018), 2017.

Oda, T., Maksyutov, S., and Elvidge, C. D.: Disaggregation of national fossil fuel CO_2 emissions using a global power plant database and DMSP nightlight data, Proceedings of the Asia Pacific Advanced Network, 30, 220–229, 2010.

Oda, T., Ganshin, A., Saito, M., Andres, R. J., Zhuravlev, R., Sawa, Y., Fisher, R. E., Rigby, M., Lowry, D., Tsuboi, K., Matsueda, H., Nisbet, E. G., Toumi, R., Lukyanov, A., and Maksyutov, S.: The use of a high-resolution emission dataset in a Global Eulerian-Lagrangian coupled model, Lagrangian Modeling of the Atmosphere, AGU Geophysical monograph series, edited by: Lin, J., Brunner, D., Gerbig, C., Stohl, A., Luhar, A., and Webley, P., American Geophysical Union, Washington, DC, https://doi.org/10.1029/2012GM0012632012, 2012.

Oda, T., Ott, L., Topylko, P., Halushchak, M., Bun, R., Lesiv, M., Danylo, O. and Horabik-Pyzel, J.: Uncertainty associated with fossil fuel carbon dioxide (CO_2) gridded emission datasets, in: Proceedings, 4th International Workshop on Uncertainty in Atmospheric Emissions, 7–9 October 2015, Krakow, Poland. Systems Research Institute, Polish Academy of Sciences, Warsaw, Poland, 124–129, ISBN 83-894-7557-X, 2015.

Oda, T., Lauvaux, T., Lu, D., Rao, P., Miles, N. L., Richardson, S. J., and Gurney, K. J.: On the impact of granularity of space-based urban CO_2 emissions in urban atmospheric inversions: A case study for Indianapolis, IN, Elem. Sci. Anth., 5, 28, https://doi.org/10.1525/elementa.146, 2017.

Olsen, S. C., Wuebbles, D. J., and Owen, B.: Comparison of global 3-D aviation emissions datasets, Atmos. Chem. Phys., 13, 429–441, https://doi.org/10.5194/acp-13-429-2013, 2013.

Peters, W., Jacobson, A. R., Sweeney, C., Andrews A. E., Conway, T. J., Masrie, K., Miller, J. B., Bruhwiler, L. M., Petron, G., Hirsch, A. I., Worthy, D. E., van der Werf, G. R., Randerson, J. T., Wennberg, P. O., Krol, M. C., and Tans, P. P.: An atmospheric perspective on North American carbon dioxide exchange: CarbonTracker, P. Natl. Acad. Sci. USA, 104, 18925–18930, 2007.

Peylin, P., Law, R. M., Gurney, K. R., Chevallier, F., Jacobson, A. R., Maki, T., Niwa, Y., Patra, P. K., Peters, W., Rayner, P. J., Rödenbeck, C., van der Laan-Luijkx, I. T., and Zhang, X.: Global atmospheric carbon budget: results from an ensemble of atmospheric CO_2 inversions, Biogeosciences, 10, 6699–6720, https://doi.org/10.5194/bg-10-6699-2013, 2013.

Raupach, M. R., Rayner, P. J., and Paget, M.: Regional variations in spatial structure of nightlights, population density and fossil-fuel CO_2 emissions, Energ. Policy, 38, 4756–4764, https://doi.org/10.1016/j.enpol.2009.08.021, 2010.

Rayner, P. J., Raupach, M. R., Paget, M., Peylin, P., and Koffi, E.: A new global gridded data set of CO_2 emissions from fossil fuel combustion: Methodology and evaluation, J. Geophys. Res., 115, D19306, https://doi.org/10.1029/2009JD013439, 2010.

Román M. O., and Stokes, E. C.: Holidays in Lights: Tracking cultural patterns in demand for energy services, Earth's Future, 3, 182–205, https://doi.org/10.1002/2014EF000285, 2015.

Saeki, T., Maksyutov, S., Sasakawa, M., Machida, T., Arshinov, M., Tans, P., Conway, T. J., Saito, M., Valsala, V., Oda, T., Andres, R. J., and Belikov, D.: Carbon flux estimation for Siberia by inverse modeling constrained by aircraft and tower CO_2 measurements, J. Geophys. Res.-Atmos., 118, 1100–1122, https://doi.org/10.1002/jgrd.50127, 2013.

Schneising, O., Heymann, J., Buchwitz, M., Reuter, M., Bovensmann, H., and Burrows, J. P.: Anthropogenic carbon dioxide source areas observed from space: assessment of regional enhancements and trends, Atmos. Chem. Phys., 13, 2445–2454, https://doi.org/10.5194/acp-13-2445-2013, 2013.

Shirai, T., Ishizawa, M., Zhuravlev, R., Ganshin, A., Belikov, D., Saito, M., Oda, T., Valsala, V., Gomez-Pelaez, A. J., Langenfelds, R., and Maksyutov, S.: A decadal inversion of CO_2 using the Global Eulerian-Lagrangian Coupled Atmospheric model (GELCA): Sensitivity to the ground-based observation network, Tellus B, 69, 1291158, https://doi.org/10.1080/16000889.2017.1291158, 2017.

Takagi H., Saeki, T., Oda, T., Saito, M., Valsala, V., Belikov, D., Saito, R., Yoshida, Y., Morino, I., Uchino, O., Andres, R. J., Yokota, T., and Maksyutov, S.: On the benefit of GOSAT ob-

servations to the estimation of regional CO_2 fluxes, SOLA, 7, 161–164, 2009.

Tans, P. P., Fung, I. Y., and Enting, I. G.: Observational constraints on the global atmospheric CO_2 budget, Science, 247, 1431–1438, 1990.

Thompson, R. L., Patra, P. K., Chevallier, F., Maksyutov, S., Law, R. M., Ziehn, T., Laan-Luijkx, I. T., Peters, W., Ganshin, A., Zhuravlev, R., Maki, T., Nakamura, T., Shirai, T., Ishizawa, M., Saeki, T., Machida, T., Poulter, B., Canadell, J. G., and Ciais, P.: Top-down assessment of the Asian carbon budget since the mid 1990s, Nat. Commun., 7, 10724, https://doi.org/10.1038/ncomms10724, 2016.

Vogel, F., Tiruchittampalam, B., Theloke, J., Kretschmer, R., Gerbig, C., Hammer, S., and Levin, I.: Can we evaluate a fine-grained emission model using high-resolution atmospheric transport modelling and regional fossil fuel CO_2 observations?, Tellus B, 65, 18681, https://doi.org/10.3402/tellusb.v65i0.18681, 2013.

Wheeler, D. and Ummel, K.: Calculating CARMA: Global Estimation of CO_2 Emissions From the Power Sector, available at: https://www.cgdev.org/publication/calculating-carma-global-estimation-co2- emissions-power-sector-working-paper-145 (last access: 10 January 2018), 2008.

Woodard, D., Branham, M., Buckingham, G., Hogue, S., Hutchins, M., Gosky, R., Marland, G., and Marland, E.: A spatial uncertainty metric for anthropogenic CO_2 emissions, Greenhouse Gas Meas. Manage., 4, 139–160, https://doi.org/10.1080/20430779.2014.1000793, 2015.

Yokota, T., Yoshida, Y., Eguchi, N., Ota, Y., Tanaka, T., Watanabe, H., and Maksyutov, S.: Global concentrations of CO_2 and CH_4 retrieved from GOSAT: First preliminary results, SOLA, 5, 160–163, https://doi.org/10.2151/sola.2009-041, 2009.

Zhang, X., Gurney, K. R., Rayner, P., Liu, Y., and Asefi-Najafabady, S.: Sensitivity of simulated CO_2 concentration to regridding of global fossil fuel CO_2 emissions, Geosci. Model Dev., 7, 2867–2874, https://doi.org/10.5194/gmd-7-2867-2014, 2014.

Ziskin, D., Baugh, K., Hsu, F.-C., Ghosh, T., Elvidege, C.: Methods Used For the 2006 Radiance Lights, Proc. of the 30th Asia-Pacific Advanced Network Meeting, 131–114, 2010.